NASA TECHNICAL NOTE

NASA TN D-7523

NASA TN D-7523

HIGH-TEMPERATURE DIELECTRIC PROPERTIES OF CANDIDATE SPACE-SHUTTLE THERMAL-PROTECTION-SYSTEM AND ANTENNA-WINDOW MATERIALS

by Melvin C. Gilreath and Stark L. Castellow, Jr.

Langley Research Center
Hampton, Va. 23665

NATIONAL AERONAUTICS AND SPACE ADMINISTRATION • WASHINGTON, D. C. • JUNE 1974

1. Report No.	2. Government Accession No.	3. Recipient's Catalog No.
NASA TN D-7523		

4. Title and Subtitle	5. Report Date
HIGH-TEMPERATURE DIELECTRIC PROPERTIES OF CANDIDATE SPACE-SHUTTLE THERMAL-PROTECTION-SYSTEM AND ANTENNA-WINDOW MATERIALS	June 1974
	6. Performing Organization Code
7. Author(s)	8. Performing Organization Report No.
Melvin C. Gilreath and Stark L. Castellow, Jr.	L-9323
	10. Work Unit No. 502-33-83-01
9. Performing Organization Name and Address	11. Contract or Grant No.
NASA Langley Research Center Hampton, Va. 23665	
	13. Type of Report and Period Covered
12. Sponsoring Agency Name and Address	Technical Note
National Aeronautics and Space Administration Washington, D.C. 20546	14. Sponsoring Agency Code

15. Supplementary Notes

16. Abstract

An experimental program was conducted to measure the dielectric properties of several candidate space-shuttle antenna-window and thermal-protection-system (TPS) materials from ambient to approximately 1473 K. The results obtained during this measurement program are presented. A description of the high-temperature-measurement technique used is given. Several problem areas associated with the low-density reusable surface insulation (RSI) materials are discussed.

The dielectric properties as a function of temperature of other dielectric materials being considered for possible space-shuttle applications are also presented.

17. Key Words (Suggested by Author(s))	18. Distribution Statement
Space-shuttle thermal-protection-system materials High-temperature dielectric properties	Unclassified – Unlimited STAR Category 07

19. Security Classif. (of this report)	20. Security Classif. (of this page)	21. No. of Pages	22. Price*
Unclassified	Unclassified	53	$3.75

*For sale by the National Technical Information Service, Springfield, Virginia 22151

HIGH-TEMPERATURE DIELECTRIC PROPERTIES OF CANDIDATE SPACE-SHUTTLE THERMAL-PROTECTION-SYSTEM AND ANTENNA-WINDOW MATERIALS

By Melvin C. Gilreath and Stark L. Castellow, Jr.
Langley Research Center

SUMMARY

An experimental program was conducted to measure the dielectric properties of several candidate space-shuttle antenna-window and thermal-protection-system (TPS) materials from ambient to approximately 1473 K. The results obtained during this measurement program are presented. A description of the high-temperature-measurement technique used is given. Several problem areas associated with the low-density reusable surface insulation (RSI) materials are discussed.

The dielectric properties as a function of temperature of other dielectric materials being considered for possible space-shuttle applications are also presented.

INTRODUCTION

Several of the space-shuttle-orbiter antennas must be located on the forward lower portion of the vehicle to provide the required radiation patterns. These antennas and the orbiter must be thermally protected from reentry-surface temperatures exceeding 1473 K. In an attempt to satisfy the space-shuttle thermal protection requirements, several nonmetallic external reusable surface insulation (RSI) materials have been developed. If such a material is used for the thermal-protection system (TPS), its use also for thermal protection of the antennas would be desirable. Generally, the thermal protection material covering antennas should preferably have a low value of both dielectric constant and loss tangent. Also, these properties should not change appreciably as a function of temperature. This investigation was conducted to determine the dielectric properties of the candidate materials over the temperature range to which they could be exposed during a shuttle reentry. No attempt was made in this investigation to determine the amount of change that could be tolerated in the dielectric properties and still maintain acceptable antenna performance. In addition to the thermal-protection-system (TPS) materials, several state-of-the-art antenna-window materials were also evaluated for possible use if the TPS materials were found to be unacceptable as antenna covers. Other materials being considered for possible reusable surface insulation (RSI) shock mounting or antenna insulation materials were evaluated but over a lower temperature range.

SYMBOLS

a_s wide dimension of test sample, cm

a_w wide dimension of waveguide, cm

b_s narrow dimension of test sample, cm

b_w narrow dimension of waveguide, cm

d_s length of test sample, cm

f frequency, Hz

$f_{r,l}$ resonant frequency of loaded cavity

$f_{r,0}$ resonant frequency of unloaded cavity

Q_l quality factor of loaded cavity at resonance

Q_0 quality factor of unloaded cavity at resonance

T temperature, K (except in the program inputs, where ^oC were used)

$\tan \delta$ loss tangent of dielectric medium

$\tan \delta_w$ loss tangent of empty waveguide

$\tan \delta_2$ loss tangent of waveguide and test sample

X_0 distance from face of test sample to first minimum

X_1 node position with empty waveguide

X_2 node position with test sample in waveguide

$\Delta X = \Delta X_2 - \Delta X_1$

ΔX_1 node width, 3 dB above the minimum in empty waveguide

ΔX_2 node width, 3 dB above the minimum with test sample in waveguide

α_s average coefficient of thermal expansion of test sample

α_w coefficient of thermal expansion of waveguide

β_2 imaginary part of the propagation constant of wave in sample within waveguide

ϵ_r relative dielectric constant

λ_c cut-off wavelength of waveguide

λ_g wavelength in waveguide

ρ density of material, kg/m^3

MATERIAL REQUIREMENTS

The material used to provide thermal protection for the antennas on a space shuttle must satisfy several operational requirements. (See refs. 1 to 3.) Among these is the requirement for the material to withstand repeated exposure to the high temperatures experienced during reentry without serious degradation of its dielectric properties. Contours of predicted maximum surface temperatures which the shuttle orbiter is expected to encounter during reentry are presented in figure 1 (from ref. 1). Note that the temperatures as given in reference 1 were Fahrenheit, whereas in figure 1, they are Kelvin. These peak temperatures and the heating rates are less than those experienced on previous spacecraft (for example, Apollo) during earth reentry; however, the duration of the maximum shuttle heating is much longer, as shown in figure 2 (from ref. 4). Again, note change in temperatures from Fahrenheit to Kelvin. The calculations presented in figure 2 were performed for a forward bottom-center-line antenna location where an emittance of 0.8 was assumed for the RSI material on a high-cross-range orbiter.

CANDIDATE MATERIALS

The materials that were evaluated during this investigation are listed in table I. Eighteen materials were evaluated, of which seven were antenna-window materials, seven were TPS materials, and four were materials being considered for other applications. The antenna-window materials consisted of boron nitrides (that is, hot pressed boron nitride, isotropic pyrolytic boron nitride), silicas (that is, slip-cast fused silica, silica

composites), aluminum phosphate foam, and a low density silicone ablative material (SLA-220 V H/C). The ablative material was evaluated because of the possibility that an ablative TPS might be used on the first vehicle if the RSI development has not progressed sufficiently by time of first launch.

The TPS materials were primarily RSI materials of a silica (namely, LI-900, LI-1500) or fibrous (namely, mullite HCF, mullite MOD IA, mullite HCF MOD IIIA) composition having relatively low densities (ρ = 161 kg/m^3 to 295 kg/m^3). (See table II.) These materials are subject to moisture absorption, as well as to damage due to handling and erosion. Also, they have poor emissivity properties. Several techniques have been developed for providing waterproofing and erosion and handling resistance. One approach has been to apply thin ceramic-like surface coatings from 0.254 mm to 0.762 mm thick. Additives to these surface coatings have achieved normal emittance values of 0.8 to 0.9. Detailed descriptions of some of the RSI materials are given in references 1 to 3. The other materials included in the TPS category were a closed-porosity insulation material (CPI-35) and an ablative material (SLA-561V H/C) of a silicone and cork composition. The CPI-35 material has a density (ρ = 561 kg/m^3) somewhat higher than the other RSI materials; however, because of its closed pore structure, it is apparently less susceptible to moisture absorption than some of the other materials. The desired emissivity can also apparently be achieved by the use of high-emissivity additives to the bulk properties of the material so that the surface-coating requirement is eliminated. The ablative TPS material (SLA-561V H/C) having a density of 240 kg/m^3 was evaluated because it was being considered as a possible backup TPS for the orbiter.

The remaining materials are those being considered for other space-shuttle applications. The rubber compounds (namely, L-4350, RL-1973, S-105) are being evaluated as possible mounting or attachment materials for the RSI panels. Dynaquartz is being considered for use as an insulation material over the antennas. Since these materials are being considered for applications requiring them to be placed over or near antennas and could affect the antenna performance, a determination of their dielectric properties was necessary.

DIELECTRIC PROPERTY MEASUREMENTS

Room Temperature

No published data were available on the room-temperature dielectric properties of several of the candidate materials and this information was required before an accurate determination of the test-sample size for the high-temperature tests could be made. Therefore, each candidate material was evaluated at room temperature by utilizing rectangular cavities to determine its dielectric constant and loss tangent. Transverse

electric (TE_{101}) dominant mode cavities having unloaded resonant frequencies of 8 to 15 GHz were used for the measurements. One of the test cavities with some typical test samples is shown in figure 3.

The dielectric properties were determined by measuring the resonant frequency and the associated quality factor for both the unloaded and loaded cavity conditions. From reference 5,

$$\epsilon_r = \left(\frac{f_{r,0}}{f_{r,l}}\right)^2 \tag{1}$$

and

$$\tan \delta = \frac{1}{Q_l} - \frac{1}{Q_0}\left(\frac{f_{r,0}}{f_{r,l}}\right)^{1/2} \tag{2}$$

where $f_{r,0}$ and Q_0 are the unloaded cavity parameters, and $f_{r,l}$ and Q_l are the loaded parameters. The resonant frequencies were measured by an interpolation method (ref. 6, pp. 386-389). The response curves of the cavities were measured by the substitution method, also given in reference 6 (pp. 403-405). The dielectric constant values obtained by this technique were then used to determine the test-sample sizes needed for the high-temperature measurements.

High-Temperature Measurements

Measurement technique.- The dielectric properties of most candidate materials were measured from room temperature up to 1473 K by the short-circuited waveguide technique (ref. 7). The basic measurement method is to determine the standing wave node positions and 3-dB node widths of a short circuited waveguide with and without the presence of the test sample as shown in figures 4(a) and 4(b). It was shown in reference 7 that for loss tangents less than 0.1, the relative dielectric constant is determined by

$$\epsilon_r = \frac{\frac{1}{\lambda_c^2} + \frac{(\beta_2 d_s)^2}{(2\pi d_s)^2}}{\frac{1}{\lambda_c^2} + \frac{1}{\lambda_g^2}} \tag{3}$$

where

λ_c waveguide cutoff wavelength

β_2 imaginary part of the propagation constant of the wave in the sample within the waveguide

d_s sample length

λ_g waveguide wavelength

The value of $\beta_2 d_s$ is determined from the relation

$$\frac{\tan \beta_2 d_s}{\beta_2 d_s} = -\frac{\lambda_g \tan \frac{2\pi X_0}{\lambda_g}}{2\pi d_s} \tag{4}$$

where X_0, the distance from face of test sample to first minimum, is

$$X_0 = \frac{n\lambda_g}{2} - \left|X_2 - X_1\right| - d_s \tag{5}$$

The solution of equation (4) for $\beta_2 d_s$ is multivalued and will give several values for ϵ_r. If the correct one cannot be selected by previous knowledge of the material (that is, approximate dielectric constant), a second measurement using a sample of different length d_s is necessary. The loss tangent of the waveguide and sample is calculated by the equation (from ref. 7):

$$\tan \delta_2 = \frac{\Delta X}{ds}\left[\frac{\frac{1}{\lambda_c^2} + \frac{1}{\lambda_g^2} - \frac{1}{\lambda_c^2 \epsilon_r}}{\frac{1}{\lambda_c^2} + \frac{1}{\lambda_g^2}}\right]\left[\frac{\beta_2 d_s\left(1 + \tan^2 \frac{2\pi X_0}{\lambda_g}\right)}{\beta_2 d_s\left(1 + \tan^2 \beta_2 d_s\right) - \tan \beta_2 d_s}\right] \tag{6}$$

where $\Delta X = \Delta X_2 - \Delta X_1$ is the difference in minimum node widths with and without the test sample in place. Since some dissipation is always present in the walls of the waveguide, a measurement of the node width includes those losses together with the dielectric losses. Consequently, the loss due to the section of waveguide must be determined and subtracted from the value found for the waveguide and sample from equation (6). The loss tangent of the empty waveguide can be determined from equation (6) after measuring ΔX_1. In this case ϵ_r would be unity, d_s would be the distance from the measured minimum to the shorted end of the waveguide, and both $\tan \frac{2\pi X_0}{\lambda_g}$ and $\tan \beta_2 d_s$ would be very large. Then, equation (6) gives for the loss tangent of the waveguide:

$$\tan \delta_w = \frac{\Delta X_1}{d_s}\left(\frac{1}{1 + \frac{\lambda_g^2}{\lambda_c^2}}\right) \tag{7}$$

Approximations were necessary in order to reduce the equations for the dielectric constant and loss tangent to the simplified forms presented in equations (3) and (6). These approximations were verified (ref. 7) by numerical calculations and for loss tangents less than 0.1 the calculation of the dielectric constant can be made to an accuracy of approximately ±1 percent. The accuracy of the approximation increases with decreasing loss tangent. Similar accuracy is also obtained in the calculation of $\tan \delta_2$.

Prior to determination of the dielectric properties of the candidate materials as a function of temperature, corrections must be included in the calculations to account for changes in the waveguide and sample sizes as a function of temperature. Changes in the sample and waveguide dimensions (that is, b_s, d_s, a_w, and b_w) due to temperature changes can produce changes in λ_c, λ_g, β_2, X_0, X_1, X_2, ΔX_1, and ΔX_2 which are used in the calculation of ϵ_r and $\tan \delta$. Therefore, thermal expansion coefficients for both the platinum-rhodium sample holder and the test samples must be included in the calculations to compensate for any changes due to thermal expansion of these components during the high-temperature tests.

Calculations.- The dielectric constant and loss tangent of each candidate material were calculated by using equations (3) and (6) and a computer program similar to that presented in reference 8. Extensive reference to this program was made in preparing a program for use on the computer facilities at the Langley Research Center. The computer program listing is presented in the appendix.

The input parameters to the computer program used for performing the calculations are as follows:

(1) Temperature, T, ^{o}C

(2) Coefficient of thermal expansion of the waveguide, α_w

(3) Average coefficient of thermal expansion of the test sample, α_s

(4) Frequency, f, Hz

(5) Wide dimension of waveguide, a_w, cm

(6) Narrow dimension of waveguide, b_w, cm

(7) Narrow dimension of test sample, b_s, cm

(8) Length of test sample, d_s, cm

(9) Node position with empty waveguide, X_1

(10) Node position with test sample in waveguide, X_2

(11) Node width, ΔX_1, 3 dB above the minimum in empty waveguide

(12) Node width, ΔX_2, 3 dB above the minimum with test sample in waveguide

(13) Estimate of dielectric constant of test sample

The calculation solves equation (4) and uses the first five solutions to substitute into equation (3). The input estimate of the dielectric constant determines which values of the relative dielectric constant and loss tangent are printed out.

Experimental.- A block diagram of the instrumentation used for the experimental measurements is shown in figure 5, and figure 6 is a photograph of the experimental set-up. The measurements were conducted at a fixed frequency of 10 GHz by using standard microwave components and measurement methods. The test sample holder was a short-circuited high-temperature waveguide constructed from a platinum-rhodium alloy. The high-temperature waveguide and test samples were inserted in a tubular furnace for heating from ambient up to a maximum temperature of 1473 K.

Dielectric sample.- The relative size and shape of the test sample required for the high-temperature measurements are shown in figure 7. The test sample must fit inside the end of the platinum-rhodium waveguide test section which has an internal cross section of 1.0160 cm by 2.2860 cm. The transverse dimensions of the sample should be 0.005 cm less than those of the test section to allow for inserting and removing the sample. The front and back surfaces should be parallel to within 0.001 cm and perpendicular to the axis of the waveguide. The length d_s of the sample depends upon the test frequency, waveguide wavelength, and an estimate of the relative dielectric constant.

Several different techniques or methods had to be used to prepare the test samples. Also, minor differences were observed in samples of the same materials. Some of the more dense antenna-window materials (for example, SCFS, silica composites) had to be machined by using diamond-tipped tools. The low-density RSI test samples were prepared by more conventional machining techniques except where it was necessary to prepare a sample having the ceramic-like surface coating. Diamond-tipped tools were required to machine this type of coating accurately. Test samples were stored in plastic bags after machining to reduce their exposure to moisture prior to testing. In addition to being stored in plastic bags, those samples indicated in table II were oven dried to reduce the moisture content before measurements of their dielectric properties were obtained.

Measurement procedure.- A calibration of the system with no test sample must be made to determine the node position X_1 and node width ΔX_1 as a function of temperature before any material samples can be evaluated. During the high-temperature tests the test frequency of 10 GHz was maintained to within 1 part in 10^8 per hour. The input power was monitored and maintained at the same level for all tests.

The high-temperature waveguide was placed inside the tubular furnace and a measurement of X_1 and ΔX_1 was obtained with the waveguide at room temperature; then, these measurements were repeated as a function of temperature in increments of 100 K from 473 K up to 1473 K. The furnace was allowed to remain at each temperature setting approximately 30 minutes before data were recorded. Once the furnace test

section had stabilized at the desired temperature, the temperature controls maintained this temperature to within ±1 K. Two thermocouples were used to monitor the temperatures of the furnace test section and the end of the waveguide where the test sample is placed. This same procedure was used to measure all the candidate materials; however, some materials were evaluated only at lower temperatures because of their limited temperature capability.

Correction for undersize test sample.- In general, it is desirable to insert the test sample into the waveguide so that there is no clearance between it and the waveguide; however, the test sample was usually machined slightly undersize to facilitate its insertion into and removal from the waveguide. Because the sample does not precisely fit the waveguide containing it, as shown in figure 8, the measured dielectric properties are in error and must be corrected. The equations used for making these corrections (ref. 5, p. 39) for the rectangular waveguide are repeated herein. A small clearance between the short wall of the rectangular waveguide and the sample can usually be neglected, since the electric field is almost zero in this region. The equations given are general and are based on approximations which are valid only when $\tan \delta \leqq 0.1$. The subscripts m and c denote "measured" and "corrected," respectively. The corrected values for the dielectric constant and loss tangent are given by

$$\epsilon'_c = \epsilon'_m \frac{b_s}{b_w - (b_w - b_s)\epsilon'_m} \tag{8}$$

$$\tan \delta_c = \tan \delta_m \frac{b_w}{b_w - (b_w - b_s)\epsilon'_m} \tag{9}$$

EXPERIMENTAL RESULTS AND DISCUSSION

Room Temperature

The results of the dielectric constant and loss tangent measurements made at room temperature by using rectangular cavities are presented in tables II and III. Most of the test samples were heated prior to being measured to reduce the moisture content; however, some materials (that is, rubber compounds, ablators) were not heated prior to the dielectric property measurements since they are suitable only for low-temperature operation or short exposure times, and any heating could alter their dielectric properties. Table II presents the dielectric property data obtained for all the materials evaluated at room temperature and also includes the measured material densities. The frequencies at which the measurements were made changed for each material because a different dielectric constant produced a different resonant frequency of the test cavity.

In order to demonstrate the effect of moisture content on the dielectric properties of the materials, several materials were measured both before and after drying, and these results are presented in table III. The drying produced very little change in the dielectric constant of the materials; however, the loss tangent improved considerably for some materials (that is, IPBN, AS-3DX).

The room-temperature results presented for the materials after drying were compared with published data (refs. 9 to 11) where available. The dielectric constant and loss tangent data presented herein, which could be compared with existing data, is within 3.5 percent in ϵ_r and 225 percent in $\tan \delta$ of that data. Density variations, different test frequencies, and drying techniques could account for some of the differences.

The dielectric constants determined from these room-temperature measurements were used to calculate the length d_s of the test samples needed for the high-temperature tests.

High Temperature

The dielectric constants and loss tangents of most candidate materials were measured at 10 GHz as a function of temperature from ambient up to 1473 K. The results of these measurements are presented in figure 9. Previously published data from references 9 to 12 are also included in figure 9 for some materials.

Slip-cast fused silica (SCFS) was used initially as the calibration material and the final results obtained for this material are presented in figure 9(a). The data presented for SCFS represents at least five different tests and more than one test sample of material. The results obtained for this material agree to within 1.5 percent in ϵ_r and within 200 percent in $\tan \delta$ of those obtained previously (refs. 10 and 11). These results indicated that the accuracies of the measurements and calculations were acceptable.

Dielectric properties for the other antenna-window materials as a function of temperature are presented in figures 9(b) to 9(g). Figure 9(b) shows the data obtained for the hot pressed boron nitride (HD-0092) material and the dielectric constant values agree to within 1 percent of published data (ref. 12). The measured loss tangent data, however, differ from published data by as much as 1100 percent at room temperature and decrease to less than a 74-percent difference at 1473 K. Published data for this material were obtained after drying the test sample in a vacuum oven, whereas the data obtained in the present investigation were obtained after the test samples were dried at atmospheric pressure. These drying processes could account for some of the difference in the loss tangent data. After the high-temperature tests of this material, a deposit was always left on the waveguide shorting plate and on the inside surface of the waveguide in the area where the test sample was located. This deposit was apparently boric oxide (B_2O_3), and

in some cases the test specimen would be fused to the shorting plate during the deposit formation. When the shorting plate was removed after the high-temperature test, a portion of the test sample would sometimes adhere to it, as shown in figure 10, and the test sample would be destroyed, so that further evaluation of that sample was not possible.

Results for isotropic pyrolytic boron nitride (IPBN) are presented in figure 9(c) with the dielectric constant values being within 1 percent at room temperature and 3 percent at 1373 K of data obtained from the manufacturer; however, a large difference in the loss-tangent data is obtained at room temperature, since loss-tangent data from the manufacturer give a value of 0.00006 as compared with the measured value of 0.0015. Other values measured at the lower temperatures are considerably higher than those supplied by the manufacturer; however, better agreement was obtained at temperatures above 1000 K. At 1373 K the value supplied by the manufacturer is 0.00012 and the measured value was 0.0005. The large differences at the lower temperatures could possibly be attributed to more moisture contained in the test samples measured in this program since the manufacturer's data were obtained on samples that were dried in a vacuum oven. The IPBN test samples left a deposit on the waveguide test section and the shorting plate during the high-temperature tests similar to those experienced with the HD-0092 material. This deposit was apparently a B_2O_3 formation as before.

The results obtained for the aluminum phosphate foam ($AlPO_4$) material are presented in figure 9(d).

Two silica composite materials were evaluated and the dielectric properties for those materials are presented in figures 9(e) and 9(f), and photographs of samples of these materials are shown in figures 11(a) and 11(b).

The results obtained for the silicone ablative antenna window material (SLA-220V H/C) are presented in figure 9(g). This material was developed primarily for high-impulse heating applied to only one surface and is not suitable for exposure to high soak temperatures. It was therefore evaluated up to a maximum test temperature of only 773 K. The dielectric constant changed very little until the temperature exceeded 673 K and then it decreased slightly. This small decrease was apparently due to shrinkage of the test sample during the temperature soaking which would indicate a lower dielectric constant. The loss tangent was 0.005 at room temperature, decreased to 0.0035 at 473 K and 573 K, and then increased slightly to approximately 0.006 at 773 K.

Dynaquartz, a low-density insulation material being considered for possible applications over or near the space-shuttle-orbiter antennas, was measured as a function of temperature and the results obtained are presented in figure 9(h).

Several RSI materials were evaluated, and the results obtained for these materials are presented in figures 9(i) to 9(m). Figure 9(i) shows the results obtained for the all

silica LI-1500 material. Measurements were made of samples having two different densities and the data show the effect of the density change on the dielectric constant. The data show very little change in ϵ_r as a function of temperature over the range investigated. The loss tangent increased from approximately 0.0005 at room temperature up to 0.0016 at 1473 K. These data are for the uncoated test samples; however, test data obtained for coated samples are discussed in a subsequent section.

Figure 9(j) presents data obtained for LI-900, another all silica material. This material is basically of the same composition as the LI-1500 material except the density has been reduced.

Data obtained for mullite HCF are presented in figure 9(k). The material composition was changed and the data obtained for the new composition, mullite HCF MOD IIIA are also presented in figure 9(k). The density of the new material is somewhat higher than that of the original material which explains its higher dielectric constant. The loss tangent of the modified material is also higher over the entire temperature range. As the data indicate, the dielectric properties of this material changed considerably as a function of temperature, and this result is not a desirable property for an antenna window material; however, other factors could make the material more suitable for a particular application.

The results obtained for the other mullite material evaluated, mullite MOD IA, are presented in figure 9(l). The changes in the dielectric properties as a function of temperature of this material were much less than those for the mullite HCF materials.

The test data for the closed porosity insulation, CPI-35, are presented in figure 9(m). Two tests were conducted for the same test sample with the first test having a maximum temperature of 1273 K and the second a maximum temperature of 1473 K. The loss tangents were essentially the same for both tests; however, the dielectric constant deviated considerably at temperatures above 1073 K. It is important to note that the dielectric properties returned to the same values after cooling to room temperatures; therefore, the high-temperature cycling apparently produced no permanent change in the room-temperature performance of the material. This particular material did exhibit a large change in both the dielectric constant and loss tangent as a function of temperature, which is not desirable for an antenna-window material as previously stated.

Several rubber-compound materials were evaluated from ambient up to 473 K, and these data are presented in figures 9(n), 9(o), and 9(p). The densities of these materials range from 246 kg/m^3 to 455 kg/m^3. The dielectric properties of all the materials behaved in a similar manner as a function of temperature with both the dielectric constant and the loss tangent decreasing with increasing temperature over the range evaluated. The dielectric-constant values ranged from 1.30 to 1.68 at room temperature.

The results obtained for SLA-561V H/C, the only ablative thermal-protection-system material evaluated, are presented in figure 9(q). The dielectric constant increased from a room-temperature value of 1.302 up to 1.323 at 473 K and 573 K, then decreased to 1.272 at the maximum test temperature of 673 K. The loss tangent behaved in a similar manner, as it increased from a room-temperature value of 0.0083 up to 0.0111 at 473 K, then decreased to approximately 0.0050 at 573 K and 673 K. This apparent decrease in both the dielectric constant and loss tangent at the elevated temperatures could be attributed to shrinkage of the test sample which would produce this effect.

Most of the RSI materials require thin surface coatings (refs. 1 to 3) for the purpose of preventing moisture absorption, improving the materials' resistance to damage from both handling and erosion, and improving the emmissivity. If an RSI material with its associated surface coating is to be used over the space-shuttle antennas, the transmission properties of the surface coating, as well as those of the basic RSI material, must also be determined as a function of temperature. After the dielectric properties of all the RSI materials were determined as a function of temperature, measurements of the transmission properties of the surface coatings as a function of temperature were then made by using the shorted waveguide technique as before. The test samples were placed in the high-temperature waveguide as shown in figure 12. The length of the test sample measured within the dielectric medium was 0.75 waveguide wavelengths, and the surface coating is located at approximately an electric field maximum. This location would tend to accentuate any change in transmission loss of the surface coating as a function of temperature.

The voltage standing-wave ratio was measured and the equivalent voltage reflection coefficient was determined for the empty waveguide as a function of temperature and this value was used as a reference for comparing the RSI materials data. The data obtained for the empty short-circuited waveguide are shown in figure 13.

Four different RSI materials were evaluated, and some typical test samples of these materials with and without surface coatings are shown in figure 14. The materials evaluated were LI-900, LI-1500, mullite MOD IA, and mullite HCF MOD IIIA. The surface coating used on the LI-900 and LI-1500 materials was grey in color and designated as 0042. The mullite MOD IA and mullite HCF surface coatings evaluated were SR-2 (brown) and B-7 (black), respectively. Voltage reflection coefficients as a function of temperature for the four materials with and without surface coatings are shown in figure 13. The surface-coating effect can be determined by comparing the results obtained for a material with a surface coating with those obtained for the same material without a surface coating. As the reflection coefficient decreases, more power is being dissipated in the test sample and/or the surface coating.

The results obtained for the LI-900 and LI-1500 materials were almost identical; therefore, the data presented in figure 13 are representative of both materials. These results indicated very little change in the waveguide reflection coefficient when the 0042 surface coating was added. This small reflection-coefficient decrease at room temperature remained about the same over the entire temperature range investigated. These data indicate very little change in the transmission properties of these materials, even after the addition of the 0042 surface coating, as a function of temperature.

The addition of the SR-2 surface coating to the mullite MOD IA material changed the voltage reflection coefficient only slightly at room temperature; however, as the temperature increases the surface-coating effect becomes more apparent, as shown in figure 13. For example, at 1473 K the reflection coefficient measured for the uncoated material is 0.818 and that of the coated sample is 0.618. Therefore, the SR-2 surface coating has a considerable influence on the transmission properties of the mullite MOD IA material at elevated temperatures.

The mullite HCF MOD IIIA surface coating produced a very small voltage-reflection-coefficient change of from 0.890 to 0.884 at room temperature. The difference between the reflection-coefficient values obtained for the uncoated and coated samples increases slightly with increasing temperature, as shown in figure 13. The value obtained at 1473 K for the coated sample is 0.416 as compared to 0.495 for the uncoated sample.

The data presented in figure 13 were also used to determine an approximate transmission loss for each of the surface coatings as a function of temperature. The surface coating was located at a maximum point of the standing wave inside the waveguide and couples only to the E-field; therefore, the observed loss for the coating is four times the loss that would be measured if the same input power level were transmitted into a matched load. In order to determine the transmission loss for the surface coatings, the loss in reflected power for the sample with no surface coating as a function of temperature was determined from the voltage-reflection coefficients presented in figure 13. Similar values were determined for the samples with surface coatings. The transmission loss of each surface coating was then determined by subtracting the loss obtained for a sample with no coating from that obtained for the sample with the surface coating. One-fourth of this difference should be the transmission loss of the surface coating only, and these data are plotted in figure 15 as a function of temperature for the three RSI surface coatings evaluated. The transmission loss measured for the 0042 surface coating on LI-900 and LI-1500 was extremely low over the entire temperature range as shown in figure 15.

The loss determined for the SR-2 surface coating on mullite MOD IA as shown in figure 15 indicates a very small transmission loss at room temperature; however, it increases to 0.63 dB at 1473 K.

The results obtained for the B-7 surface coating on mullite HCF MOD IIIA show a very small transmission loss at room temperature. The data obtained for this surface coating are very similar to that of the SR-2 surface coating up through 873 K. For temperatures greater than 873 K the transmission loss of the B-7 surface coating reaches a maximum value of 0.39 dB at 1473 K.

CONCLUDING REMARKS

Results have been presented of an experimental investigation to determine the dielectric properties of several candidate space-shuttle antenna-window and thermal-protection materials.

The agreement between measured and available published data was generally very good with the major differences occurring in the loss-tangent data at the lower temperatures. Most published data were obtained with test samples that had been dried in a vacuum oven; however, the data obtained in the present investigation were for test samples that had been oven dried only at atmospheric pressure and possibly could have retained more moisture that caused the measured loss-tangent values to be higher. In an actual shuttle application the antenna-window material would normally be exposed to atmospheric conditions during portions of the flight which could produce a higher loss tangent if the material were susceptible to moisture absorption.

Several of the antenna-window materials showed relatively small changes (less than 5 percent) in the dielectric constant and low loss tangents from room temperature to 1473 K. The boron-nitride materials (that is, IPBN and HD-0092) formed what appeared to be boric oxide (B_2O_3) deposits on the surface of the test samples during the high-temperature tests, which caused the test samples to adhere to the waveguide test section. This deposit could conceivably create a problem in a shuttle antenna-window application where it might be desirable to remove the window from surrounding materials after exposure to a high-temperature shuttle entry. These materials should be investigated in an environment more closely simulating the shuttle-orbiter entry conditions prior to their use on the shuttle.

The LI-900 and LI-1500 reusable surface insulation materials exhibited very little change in the dielectric constant, and the loss tangent remained below 0.002 from room temperature to 1473 K. The 0042 surface coating on LI-900 and LI-1500 produced a very small transmission loss at 10 GHz over the temperature range investigated. The dielectric properties of these materials and the very low transmission loss produced by the 0042 surface coating indicate them to be excellent candidate antenna-window materials for the shuttle orbiter.

Some of the RSI materials evaluated were still undergoing minor changes for improving their thermal and/or mechanical properties, surface coatings, densities or other material properties; however, the results obtained for a particular material should be representative of that type of material. Small changes in the material composition should not affect the dielectric properties appreciably; however, the final RSI material selected for use as the shuttle-orbiter TPS should be evaluated to determine its dielectric properties as a function of temperature and frequency before it is used as an antenna-window material.

Langley Research Center,
National Aeronautics and Space Administration,
Hampton, Va., February 4, 1974.

APPENDIX

COMPUTER PROGRAM

```
      PROGRAM DIELTRC(INPUT,OUTPUT,TAPE10=INPUT)
C     THIS PROGRAM WILL DETERMINE FIVE POSSIBLE DIELECTRIC CONSTANTS
C     AND THEIR ASSOCIATED LOSS TANGENTS FOR A SAMPLE IN A CLOSED
C     WAVE GUIDE.  INPUT TO THE PROGRAM IS IN CARD FORM AS DESCRIBED
C     BELOW
C          CARD ONE-
C            TEMP-TEMPERATURE MEASURED IN DEGREES CENTIGRADE
C            CFWG-COEFFICIENT OF THERMAL EXPANSION FOR THE WAVE GUIDE
C                 IN CENTIMETERS PER DEGREE CENTIGRADE
C            CFSMP-COEFFICIENT OF THERMAL EXPANSION OF THE SAMPLE IN
C                  CENTIMETERS PER DEGREE CENTIGRADE
C            SMPXP-THERMAL EXPANSION OF THE SAMPLE FOR THE TEST
C                  TEMPERATURE IN CENTIMETERS PER CENTIMETER
C            FREQ-TEST FREQUENCY
C            AWG-DIMENSION OF WAVEGUIDE IN CENTIMETERS
C            BWG-DIMENSION OF WAVEGUIDE IN CENTIMETERS
C          CARD TWO-
C            BSMP-DIMENSION OF SAMPLE IN CENTIMETERS
C            DSMP-DIMENSION OF SAMPLE IN CENTIMETERS
C            X1-POSITION OF MINIMUM WITH EMPTY WAVEGUIDE
C            X2-POSITION OF MINIMUM WITH TEST SPECIMEN IN WAVE GUIDE
C            DX1-WIDTH OF NODE AT DOUBLE POWER POINTS.OR AT POWER
C                  LEVEL 3 DB ABOVE THE MINIMUM IN EMPTY WAVEGUIDE
C            DX2-WIDTH OF NODE AT DOUBLE POWER POINTS.OR AT POWER
C                  LEVEL 3 DB ABOVE THE MINIMUM WITH TEST SPECIMEM IN
C                  WAVEGUIDE
C             ESTMK-AN ESTIMATE OF THE DIELECTRIC CONSTANT OF THE
C                  TEST SPECIMEN
C     NOTE 1-EXTENSIVE REFERENCE WAS MADE TO NASA REPORT GE/EE/65-21
C     NOTE 2- ALL PARAMETERS ARE READ IN AN E11.4 FORMAT
C     NOTE 3- IF CFSMP IS USED,THE FIELD FOR SMPXP SHOULD BE LEFT BLANK
000003        DIMENSION Y(5),ELTRK(5),TNLOSS(5)
000003        REAL LAMDA,LAMDC,LAMDG
000003        COMMON/ONE/NI,PI,CNST
000003     10 READ 900,SAMPLE
000011    900 FORMAT(A10)
000011        IF(EOF,10)500,11
000014     11 READ 1000,TEMP,CFWG,CFSMP,SMPXP,FREQ,AWG,BWG
000036   1000 FORMAT(7E11.4)
000056        IF(EOF,10)500,15
000041     15 READ 1000,BSMP,DSMP,X1,X2,DX1,DX2,ESTMK
000063        IF(EOF,10)500,20
000066     20 PI=2.*ASIN(1.)
000072        PRINT 2000,TEMP,CFWG,CFSMP,SMPXP,FREQ,AWG,BWG,BSMP,DSMP,X1,X2,DX1,
             1DX2
000127        AWG=AWG*(1.+CFWG*TEMP)
000133        BWG=BWG*(1.+CFWG*TEMP)
000135        IF(CFSMP.EQ.0.)30,40
000141     30 BSMP=BSMP+BSMP*SMPXP
000143        DSMP=DSMP+DSMP*SMPXP
000145        GO TO 50
000146     40 BSMP=BSMP*(1.+CFSMP*TEMP)
000152        DSMP=DSMP*(1.+CFSMP*TEMP)
```

APPENDIX

```
000154       50 LAMDA=2.998E10/FREQ
000156          LAMDG=2.*AWG
000160          P=(LAMDA/LAMDG)**2
000162          LAMDG=LAMDA/SQRT(1.-P)
000166          PIDS=2.*PI*DSMP
000171          X=PIDS/LAMDG
000173          N=0
000173          MARK=0
000175       60 N=N+1
000177          XO=N/2-DSMP/LAMDG-ABS(X2-X1)/LAMDG
000206          IF(XO.LT.0.)GO TO 60
000210          IF(XO.GT.0.5)GO TO 200
000214          PIXO=2.*PI*XO
000215          TPIXO=TAN(PIXO)
000217          CNST=-TPIXO/X
000222          CALL FINDX(ESTMK,Y)
000224          DO 100 I=1,5
000226          DIEL=(1.-P)*((Y(I)*(LAMDG/PIDS))**2-1.)+1
000235          GAMA=(1.-(BSMP/BWG))*(DIEL-1.)
000242          IF(DIEL.GE.1..AND.DIEL.LT.2.6)DLTRK(I)=DIEL*(1.+GAMA)
000255          IF(DIEL.GE.2.6.AND.DIEL.LT.5.2)DLTRK(I)=DIEL+4.16*(1.-BSMP/BWG)
000273          IF(DIEL.GT.5.2)DLTRK(I)=DIEL+GAMA
000301          IF(DIEL.LT.1.)70,80
000306       70 DLTRK(I)=0.
000310          TNLOSS(I)=0.
000311          GO TO 100
000311       80 PKI=P/DLTRK(I)
000313          DDELX=ABS(DX2-DX1)/DSMP
000317          FQ=(Y(I)+Y(I)*TAN(PIXO)**2)/ (TAN(Y(I))**2*Y(I)-TAN(Y(I))+Y(I))
000340          TNLOSS(I)=DDELX*(1.-PKI)*FQ
000345      100 CONTINUE
000347      110 CONTINUE
000347          PRINT 2500
000353     2500 FORMAT(//8X*THERMALLY CORRECTED*)
000353          PRINT 2000,TEMP,CFWG,CFSMP,SMPXP,FREQ,AWG,BWG,BSMP,DSMP,X1,X2,DX1,
                1DX2
000411     2000 FORMAT(//15X*INPUT*//5X*TEMP =*E15.4* DEG C*/5X*CFWG =*F15.4* CM
                APER DEG C*/5X*CFSMP=*E15.4* CM PER DEG C*/5X*SMPXP=*E15.4* CM PER
                BCM*/5X*FREQ =*E15.4* HZ*/5X*AWG  =*E15.4* CM*/5X*BWG  =*
                CE15.4* CM*/5X*BSMP =*E15.4* CM*/5X*DSMP =*E15.4* CM*/5X*X1   =*E
                D15.4* CM*/5X*X2   =*E15.4* CM*/5X*DX1  =*E15.4* CM*/5X*DX2  =*
                EE15.4* CM*)
000411          PRINT 3500,SAMPLE
000417     3500 FORMAT(//* THE SAMPLE IS*3X,A10)
000417          PRINT 4000,ESTMK
000425     4000 FORMAT(//5X*THE ESTIMATED DIELECTRIC =*E15.6)
000425          IF(MARK.EQ.1)GO TO 500
000427          PRINT 3000,(I,DLTRK(I),TNLOSS(I),I=1,5)
000444     3000 FORMAT(//15X*OUTPUT*/4X*I*4X*DIELECTRIC*5X*TANLOSS*/(I5,2E15.6))
000444          GO TO 10
000445      200 PRINT 5000
000451     5000 FORMAT(/* XO COULD NOT BE DETERMINED*)
000451          MARK=1
000452          GO TO 110
000453      500 STOP
000455          END
```

APPENDIX

```
DIELTRC

PROGRAM LENGTH INCLUDING I/O BUFFERS
004764

FUNCTION ASSIGNMENTS

STATEMENT ASSIGNMENTS
10      -  000003    11      -  000014    15      -  000041    20      -  000066
30      -  000141    40      -  000146    50      -  000154    60      -  000175
70      -  000306    80      -  000311    100     -  000345    110     -  000347
200     -  000445    500     -  000453    900     -  000467    1000    -  000472
2000    -  000512    2500    -  000506    3000    -  000567    3500    -  000555
4000    -  000561    5000    -  000576

BLOCK NAMES AND LENGTHS
ONE     -  000003

VARIABLE ASSIGNMENTS
AWG     -  000671    BSMP    -  000675    BWG     -  000672    CFSMP   -  000666
CFWG    -  000665    CNST    -  000002    DDELX   -  000716    DIEL    -  000713
DLTRR   -  000646    DSMP    -  000674    DX1     -  000677    DX2     -  000700
ESTMR   -  000701    FW      -  000717    FREQ    -  000670    GAMA    -  000714
I       -  000712    LAMDA   -  000660    LAMDG   -  000661    LAMDG   -  000662
MARK    -  000706    N       -  000705    P       -  000702    PI      -  000001
PIDS    -  000703    PIXL    -  000710    PKI     -  000715    SAMPLE  -  000663
SMPXP   -  000667    TEMP    -  000664    TNLOSS  -  000653    TPIXD   -  000711
X       -  000704    XO      -  000707    X1      -  000675    X2      -  000676
Y       -  000641

START OF CONSTANTS
000457

START OF TEMPORARIES
000604

START OF INDIRECTS
000035

UNUSED COMPILER SPACE
011400
```

APPENDIX

```
000005          SUBROUTINE FINDX(ESTMK,Y)
000005          DIMENSION Y(5)
000005          COMMON/ONE/N1,PI,CNST
000005          EXTERNAL TANY
000005          E1=1.E-5
000006          E2=1.E-6
000007          DELY=.0001
000011          N=0
000011          MAX=200
000012          ESTMKR=ESTMK
000014       10 IF(ESTMK.GE.(2*N-1)*PI/2..AND.ESTMK.LE.(2*N+1)*PI/2.)20,70
000035       20 DO 60 I=1,5
000037          N1=(N-3)+I
000041          CALL ITR1(ESTMKR,DELY,TANY,E1,E2,MAX,ICODE)
000050          ICODE=ICODE+1
000052          GO TO (30,40,50),ICODE
000061       30 Y(I)=ATAN(ESTMKR)+N1*PI
000071          GO TO 60
000072       40 PRINT 1000
000076     1000 FORMAT(* FAILED TO CONVERGE IN 200 ITERATIONS*)
000076          GO TO 60
000100       50 PRINT 2000
000104     2000 FORMAT(* DERIVATIVE EQUALS ZERO*)
000104       60 CONTINUE
000110          GO TO 80
000110       70 IF(N.GT.50) GO TO 75
000114          N=N+1
000115          GO TO 10
000115       75 PRINT 3000
000121     3000 FORMAT(* ESTIMATE OUT OF RANGE*)
000121       80 CONTINUE
000121          RETURN
000122          END
```

APPENDIX

```
FINDX

SUBPROGRAM LENGTH
000171

FUNCTION ASSIGNMENTS

STATEMENT ASSIGNMENTS
10      -  000014    20      -  000035    30      -  000061    40      -  000072
50      -  000100    60      -  000104    70      -  000110    75      -  000115
80      -  000121    1000    -  000132    2000    -  000140    3000    -  000144

BLOCK NAMES AND LENGTHS
ONE     -  000003

VARIABLE ASSIGNMENTS
DELY    -  000163    ESTMKR  -  000166    E1      -  000161    E2      -  000162
I       -  000167    ICODE   -  000170    MAX     -  000165    N       -  000164
N1      -  000000001 PI      -  000001001

START OF CONSTANTS
000124

START OF TEMPORARIES
000150

START OF INDIRECTS
000160

UNUSED COMPILER SPACE
013000
```

APPENDIX

```
                FUNCTION TANY(Y)
000003          COMMON/ONE/NI,PI,CNST
000003          TANY=CNST*ATAN(Y)+CNST*NI*PI
000011          RETURN
000012          END


TANY

SUBPROGRAM LENGTH
000022

FUNCTION ASSIGNMENTS

STATEMENT ASSIGNMENTS

BLOCK NAMES AND LENGTHS
ONE     -  000003

VARIABLE ASSIGNMENTS
CNST    -  000002C01 NI      -  000000C01 PI      -  00CC01C01 TANY    -  0C0021

START OF CONSTANTS
000014

START OF TEMPORARIES
000015

START OF INDIRECTS
000021

UNUSED COMPILER SPACE
013400
```

```
CORE MAP  16.49.46.  NORMAL              CONTROL                                          000100    013376    000000    000000
   ---TIME---LOAD MODE --L1--L2------TYPE--------------USER---++---CALL-------------FWA LOAD--LWA LOAD--BLNK COMN--LENGTH--
   FWA LOADER  044331  FWA TABLES  043625
   -PROGRAM----ADDRESS-                    --LABELED---COMMON--
   DIELTRC     000103                              CNE          000100
   FINDX       005067                              CNE          000100
   TANY        005260                              ONE          000100
   SYSTEM      005302
   INPUTC      006424
   IFENDF      006535
   ASINCOS     006617
   OUTPTC      006755
   SQRT        007055
   TAN         007120
   ITR1        007231
   ACOSER      007372
   ATAN        007404
   SIO$        007500
   GETBA       011044
   KRAKER      011063
   KODER       012126
   --ENTRY-----ADDRESS-                                              REFERENCES
   DIELTRC     000104
   FINDX       005070          DIELTRC     000326

   TANY        005261          FINDX       005131

   Q8NTRY      005303          DIELTRC     000105

   SYSTEM      005522          INPUTC      006470
                               IFENDF      006610
                               ASINCOS     006711    006714
                               OUTPTC      007042
                               SQRT        007102
                               TAN         007201
                               ACOSER      007375
                               ATAN        007443
                               KRAKER      011660    011767
                               KODER       013201

   SYSTEMC     005447
   SYSTEMP     005476
   END         005571          DIELTRC     000561
                               FINDX       005212
                               TANY        005273
                               ITR1        007345

   STOP        005421          DIELTRC     000557

   EXIT        005413
```

ABNORML	005431	INPUTC	006471						
		IFENDF	006611						
		OUTPTC	007043						
		ACOOER	007376						
		KRAKER	011710						
		KUDER	013202						
SYSTEMF	005503								
INPUTC	006426	DIELTRC	000110	000112	000113	000121	000123	000125	000127
			000131	000133	000135	000137	000140	000146	000150
			000152	000154	000156	000160	000162	000164	000165
IFENDF	006536	DIELTRC	000115	000142	000167				
ASIN	006623	DIELTRC	000172						
ACOS	006620								
OUTPTC	006757	DIELTRC	000176	000200	000202	000204	000206	000210	000212
			000214	000216	000220	000222	000224	000226	000230
			000231	000454	000455	000460	000462	000464	000466
			000470	000472	000474	000476	000500	000502	000504
			000506	000510	000512	000513	000516	000520	000521
			000524	000526	000527	000534	000537	000541	000543
			000546	000552	000553				
		FINDX	005163	005164	005171	005172	005206	005207	
SORT	007056	DIELTRC	000267						
TAN	007121	DIELTRC	000321	000425	000430	000436			
ITRI	007233	FINDX	005133	005136					
ACOOER	007373	FINDX	005144						
ATAN	007405	FINDX	005151						
		TANY	005263						
CIO1.	010544								
RCL1.	010561	SYSTEM	005756						
DAT.	007502	INPUTC	006444	006500	006506	006514			
		OUTPTC	006773	007006	007014				
		KRAKER	011657	011712	011720	011731			
SIO.CTL	007730	SYSTEM	005740						
		IFENDF	006570						
INITL.	007750	SYSTEM	005736	005700					
		INPUTC	006434						
		OUTPTC	006766						

APPENDIX

```
SIO.            010014          SYSTEM      0C5702
                                INPUTC      0C6502
                                OUTPTC      0C7013

SIO.END         010515          SYSTEM      0C5753

OPEN.           010570          SYSTEM      006053

RDPRU.          010632          IFENDF      0C6571

BKSPRU.         010650          IFENDF      0C6577

ADVIN.          010655          SYSTEM      0C5752

POSFI.          010703
MVWDS.          011030
GETBA           011045          SYSTEM      005504
                                IFENDF      0C6541
                                SIO$        0C7752

KRAKER          011064          INPUTC      0C6430      006447

KODER           012127          OUTPTC      006776      006761

----UNSATISFIED EXTERNALS-----                          REFERENCES
```

INPUT

```
TEMP =      2.5000E+01  DEG C
CFWG =      8.8000E-06  CM  PER DEG C
CFSMP=      3.0000E-06  CM PER DEG C
SMPXP=      0.          CM PER CM
FREQ =      1.0000E+10  HZ
AWG  =      2.2733E+00  CM
BWG  =      1.0160E+00  CM
BSMP =      1.0109E+00  CM
DSMP =      2.3292E+00  CM
X1   =      1.3800E+01  CM
X2   =      1.2730E+01  CM
DX1  =      4.1000E-02  CM
DX2  =      1.1500E-01  CM
```

APPENDIX

THERMALLY CORRECTED

INPUT

```
TEMP =      2.5000E+01 DEG C
CFWG =      8.8000E-06 CM  PER DEG C
CFSMP=      3.0000E-06 CM PER DEG C
SMPXP=      0.         CM PER CM
FREQ =      1.0000E+10 HZ
AWG  =      2.2738E+00 CM
BWG  =      1.0162E+00 CM
BSMP =      1.0110E+00 CM
DSMP =      2.3294E+00 CM
X1   =      1.3800E+01 CM
X2   =      1.2730E+01 CM
DX1  =      4.1000E-02 CM
DX2  =      1.1500E-01 CM
```

THE SAMPLE IS RAYDESTS

THE ESTIMATED DIELECTRIC = 1.000000E+00

OUTPUT

I	DIELECTRIC	TANLOSS
1	0.	0.
2	0.	0.
3	0.	0.
4	1.573903E+00	1.296145E-02
5	3.263229E+00	7.515230E-03

INPUT

```
TEMP =      1.6000E+02 DEG C
CFWG =      8.8000E-06 CM  PER DEG C
CFSMP=      3.0000E-06 CM PER DEG C
SMPXP=      0.         CM PER CM
FREQ =      1.0000E+10 HZ
AWG  =      2.2733E+00 CM
BWG  =      1.0160E+00 CM
BSMP =      1.0109E+00 CM
DSMP =      2.3292E+00 CM
X1   =      1.3740E+01 CM
X2   =      1.2690E+01 CM
DX1  =      4.1500E-02 CM
DX2  =      7.2000E-02 CM
```

APPENDIX

THERMALLY CORRECTED

INPUT

TEMP =	1.6000E+02	DEG C
CFWG =	8.8000E-06	CM PER DEG C
CFSMP=	3.0000E-06	CM PER DEG C
SMPXP=	0.	CM PER CM
FREQ =	1.0000E+10	HZ
AWG =	2.2765E+00	CM
BWG =	1.0174E+00	CM
BSMP =	1.0114E+00	CM
DSMP =	2.3303E+00	CM
X1 =	1.3740E+01	CM
X2 =	1.2690E+01	CM
DX1 =	4.1500E-02	CM
DX2 =	7.2000E-02	CM

THE SAMPLE IS RAYBESTS

THE ESTIMATED DIELECTRIC = 1.600000E+00

OUTPUT

I	DIELECTRIC	TANLOSS
1	0.	0.
2	0.	0.
3	0.	0.
4	1.564027E+00	5.306652E-03
5	3.253047E+00	3.035868E-03

REFERENCES

1. Vance, M. W.: The Manufacture of Mullite Reusable Surface Insulation Materials for Space Shuttle. Paper presented to the Society of Manufacturing Engineers WESTEC Conference, Mar. 15, 1972.

2. Buttram, R. D.: Development of a Rigidized, Surface Insulative Thermal Protection System for Shuttle Orbiter. MSC-02567 (Contract No. NAS 9-11222), Lockheed Missiles and Space Co., Feb. 16, 1971. (Available as NASA CR-114958.)

3. Tanzilli, Richard A.: Development of an External Ceramic Insulation for the Space Shuttle Orbiter. NASA CR-112038, 1972.

4. Gilreath, M. C.; and Castellow, S. L., Jr.: High-Temperature Dielectric Properties of Several Candidate Space Shuttle Thermal Protection System and Antenna Window Materials. Proceedings of the Eleventh Symposium on Electromagnetic Windows – State of Radome Technology-1972, N. E. Poulos and J. D. Walton, Jr., eds., Georgia Inst. Technol., Aug. 1972, pp. 144-148.

5. Altschuler, H. M.: Dielectric Constant. Handbook of Microwave Measurements, Third ed., Vol. II, Max Sucher and Jerome Fox, eds., Polytech. Press of Polytech. Inst. Brooklyn, c.1963.

6. Ginzton, Edward L.: Microwave Measurements. McGraw-Hill Book Co., Inc., 1957.

7. Dakin, T. W.; and Works, C. N.: Microwave Dielectric Measurements. J. Appl. Phys., vol. 18, no. 9, Sept. 1947, pp. 789-796.

8. Sage, Glen H.: Measurement of Electrical Properties of High Temperature Radome Materials by Means of the XB 3000A Dielectrometer. M.S. Thesis, Air Force Inst. Technol., Air Univ., U.S. Air Force, Nov. 1965.

9. Place, T. M.; and Bridges, D. W.: Fused Quartz-Reinforced Silica Composites for Radomes. Proceedings of the Tenth Symposium on Electromagnetic Windows – State of Radome Technology-1970, N. E. Poulos and J. D. Walton, Jr., eds., Georgia Inst. Technol., July 1970, pp. 115-119.

10. Bassett, H. L.; and Bomar, S. H., Jr.: Dielectric Constant and Loss Tangent Measurement of High-Temperature Electromagnetic Window Materials. Proceedings of the Tenth Symposium on Electromagnetic Windows – State of Radome Technology-1970, N. E. Poulos and J. D. Walton, Jr., eds., Georgia Inst. Technol., July 1970, pp. 187-191.

11. Bomar, S. H., Jr.; and Bassett, H. L.: High-Temperature Complex Permittivity Measurements on Antenna Window Materials. Proceedings of the Eleventh Symposium on Electromagnetic Windows – State of Randome Technology-1972, N. E. Poulos and J. D. Walton, Jr., eds., Georgia Inst. of Technol., Aug. 1972, pp. 139-143.

12. Mandorf, V.; Montgomery, L. C.; and Henika, M.: Boron Nitride in Aerospace, SAMPE J., Oct./Nov. 1968, pp. 65-68.

TABLE I.- CANDIDATE MATERIALS

Material	Supplier	Application
Slip-cast fused silica, SCFS	Georgia Institute of Technology	Antenna window
Hot pressed boron nitride, HD-0092	Union Carbide Corp.	Antenna window
Isotropic pyrolytic boron nitride, IPBN	Raytheon Co.	Antenna window
Aluminum phosphate foam, $AlPO_4$	Whittaker Corp.	Antenna window
Fused quartz reinforced silica composite, AS-3DX	Philco-Ford Corp.	Antenna window
Multidirectional silica composite, Markite 3DQ	General Electric Co.	Antenna window
Silicone ablator, SLA-220V H/C	Martin Marietta Aerospace	Antenna window
Dynaquartz	Johns-Manville	Insulation/Antenna window
All silica, LI-900	Lockheed Missiles and Space Co.	Reusable surface insulation
All silica, LI-1500	Lockheed Missiles and Space Co.	Reusable surface insulation
Hardened compacted mullite fibers, mullite HCF	McDonnell Douglas Corp.	Reusable surface insulation
Hardened compacted mullite fibers, mullite HCF MOD IIIA	McDonnell Douglas Corp.	Reusable surface insulation
Mullite MOD IA	General Electric Co.	Reusable surface insulation
Closed porosity insulation, CPI-35	Grumman Aerospace Corp.	Reusable surface insulation
Cork composite, SLA-561V H/C	Martin Marietta Aerospace	Thermal protection system material
Methyl phenyl silicone sponge, L4350	Raybestos-Manhattan, Inc.	RSI shock mounting
Silicone sponge, RL-1973	Raybestos-Manhattan, Inc.	RSI shock mounting
Silicone sponge, S-105	Raybestos-Manhattan, Inc.	RSI shock mounting

TABLE II.- ROOM-TEMPERATURE PROPERTIES OF CANDIDATE MATERIALS

[Materials dried 3 to 5 hours at 473 K]

Material	Frequency, GHz	Dielectric constant, ϵ_r	Loss tangent, tan δ	Density, ρ, kg/m^3
SCFS	5.375	3.40	0.00089	1980
HD-0092	4.915	4.07	.00056	1990
IPBN	5.726	3.00	.00011	1220
$AlPO_4$	7.362	1.82	.00401	830
AS-3DX	5.841	2.88	.00612	1620
Markite 3DQ	5.555	3.19	.00057	1890
SLA-220V H/C*	12.950	1.33	.00609	250
Dynaquartz	9.260	1.15	.00050	160
LI-900	9.300	1.14	.00057	161
LI-1500	8.980, 9.230	1.22, 1.15	0.00132, 0.00134	252, 210
Mullite HCF	9.049	1.20	.00165	220
Mullite HCF MOD IIIA	8.740	1.29	.00182	295
Mullite MOD IA	9.046	1.20	.00057	185
CPI-35	7.474	1.76	.00845	561
SLA-561V H/C*	10.000	1.30	.00830	240
L-4350*	7.800	1.62	.01072	414
RL-1973*	12.960	1.33	.01280	246
S-105*	11.400	1.69	.01282	455

*Not dried.

TABLE III.- ROOM-TEMPERATURE DIELECTRIC PROPERTIES

Material	Frequency, GHz		Dielectric constant, ϵ_r		Loss tangent, tan δ	
	Before drying	After drying	Before drying	After drying	Before drying	After drying
SCFS	5.36	5.36	3.40	3.40	0.00117	0.00089
HD-0092	4.92	4.92	4.07	4.07	.00056	.00056
IPBN	5.68	5.73	3.05	3.00	.00372	.00011
$AlPO_4$	7.34	7.36	1.83	1.82	.00680	.00400
AS-3DX	5.80	5.84	2.92	2.88	.01086	.00612
Markite 3DQ	5.53	5.56	3.21	3.19	.00054	.00057
LI-1500	8.97	8.97	1.22	1.22	.00178	.00082
Mullite HCF	9.05	9.05	1.20	1.20	.00190	.00170
Mullite HCF MOD IIIA	8.74	8.74	1.29	1.29	.00192	.00182
Mullite MOD IA	9.05	9.05	1.20	1.20	.00067	.00057
CPI-35	7.46	7.46	1.76	1.76	.00370	.00750
Dynaquartz	9.26	9.26	1.15	1.15	.00091	.00050

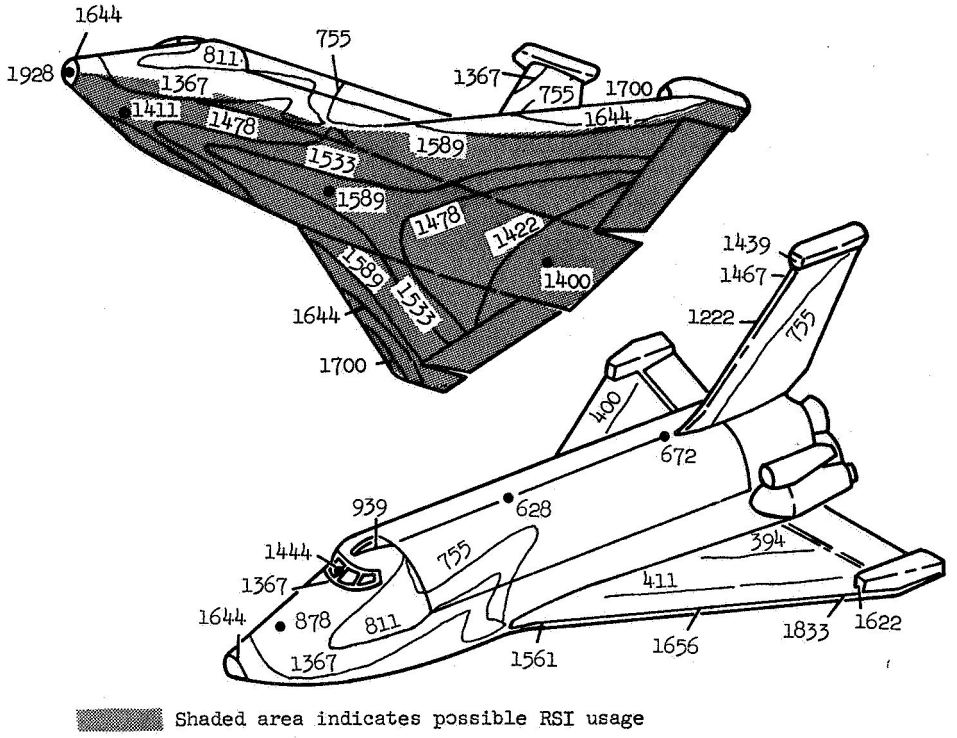

Figure 1.- Predicted maximum shuttle-orbiter-entry temperatures, K, converted from ^{o}F in reference 1.

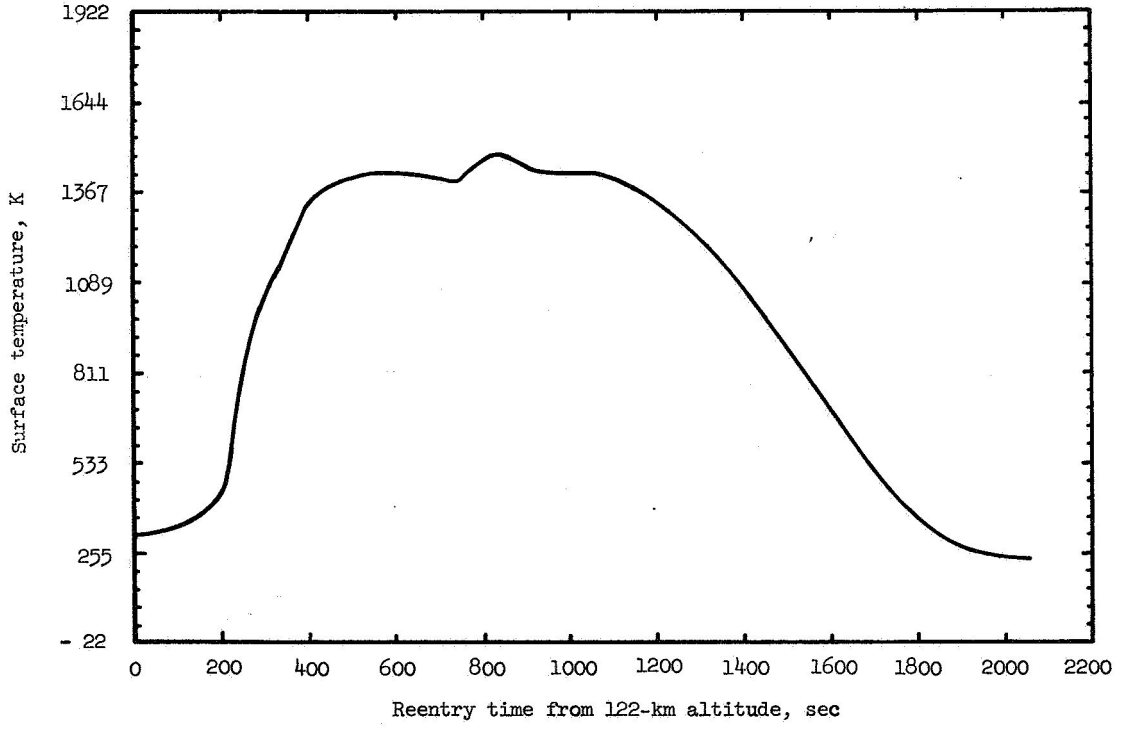

Figure 2.- Predicted RSI TPS surface-temperature profile for an antenna located on the forward bottom center line of a high-cross-range orbiter.

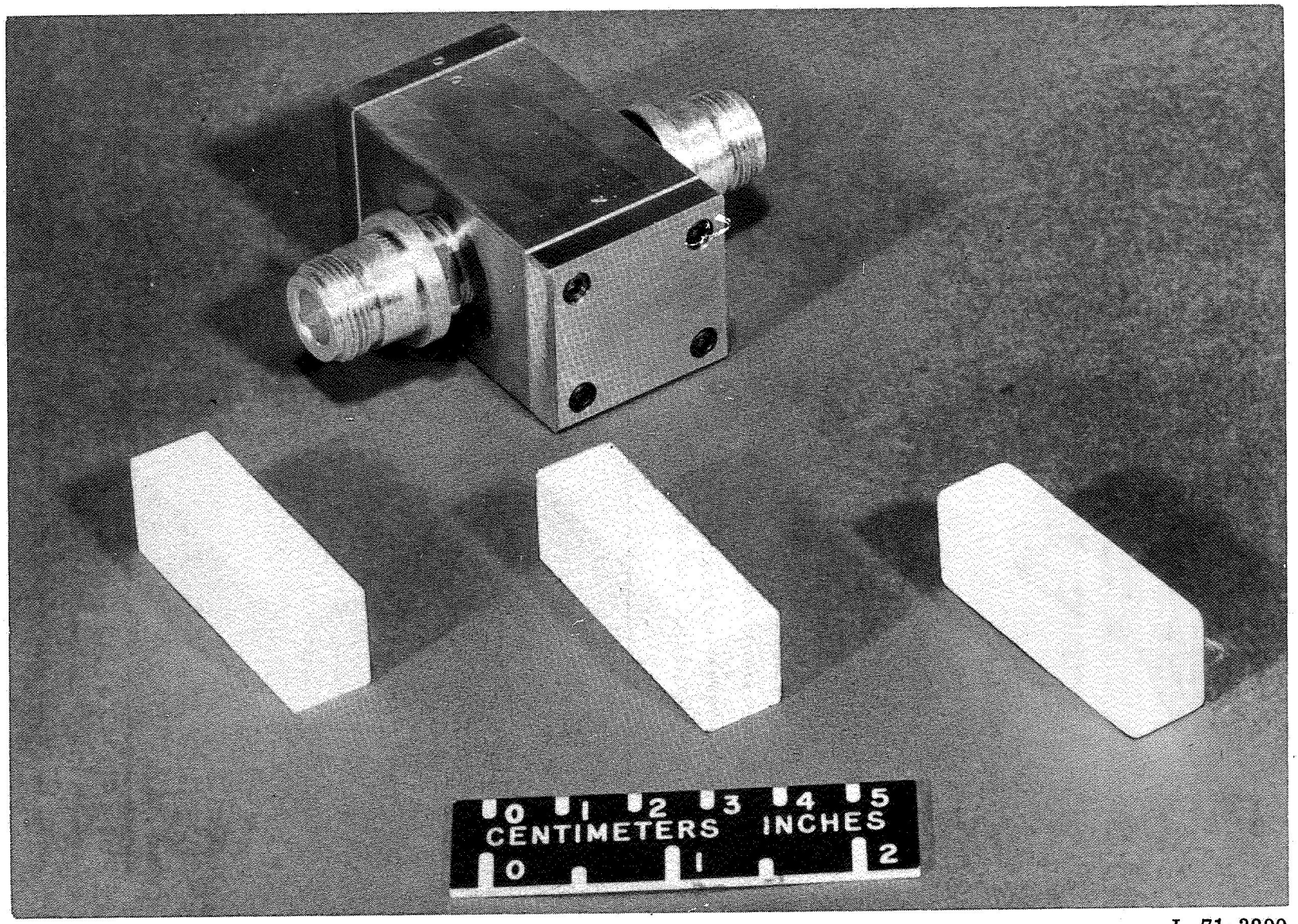

L-71-3899

Figure 3.- Rectangular cavity with typical test samples.

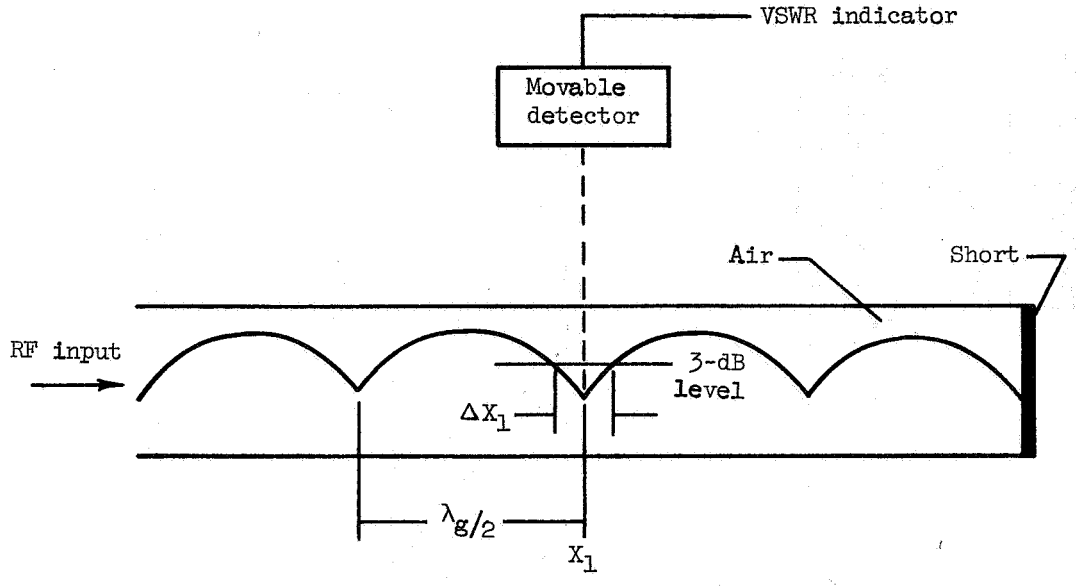

(a) No test sample.

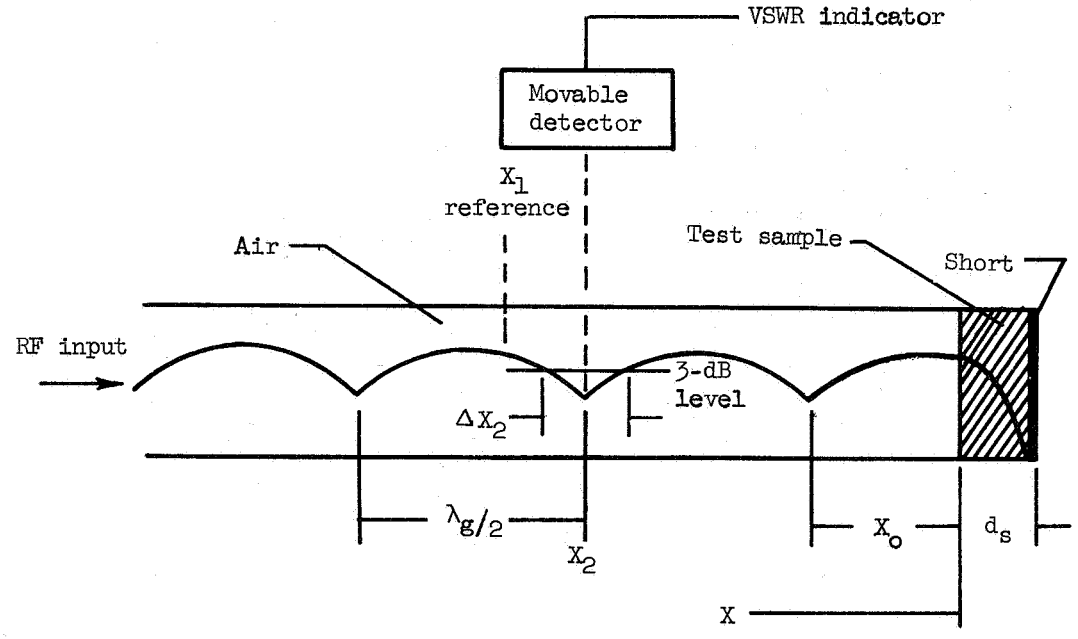

(b) With test sample.

Figure 4.- Voltage standing-wave ratio (VSWR) within short-circuited waveguide.

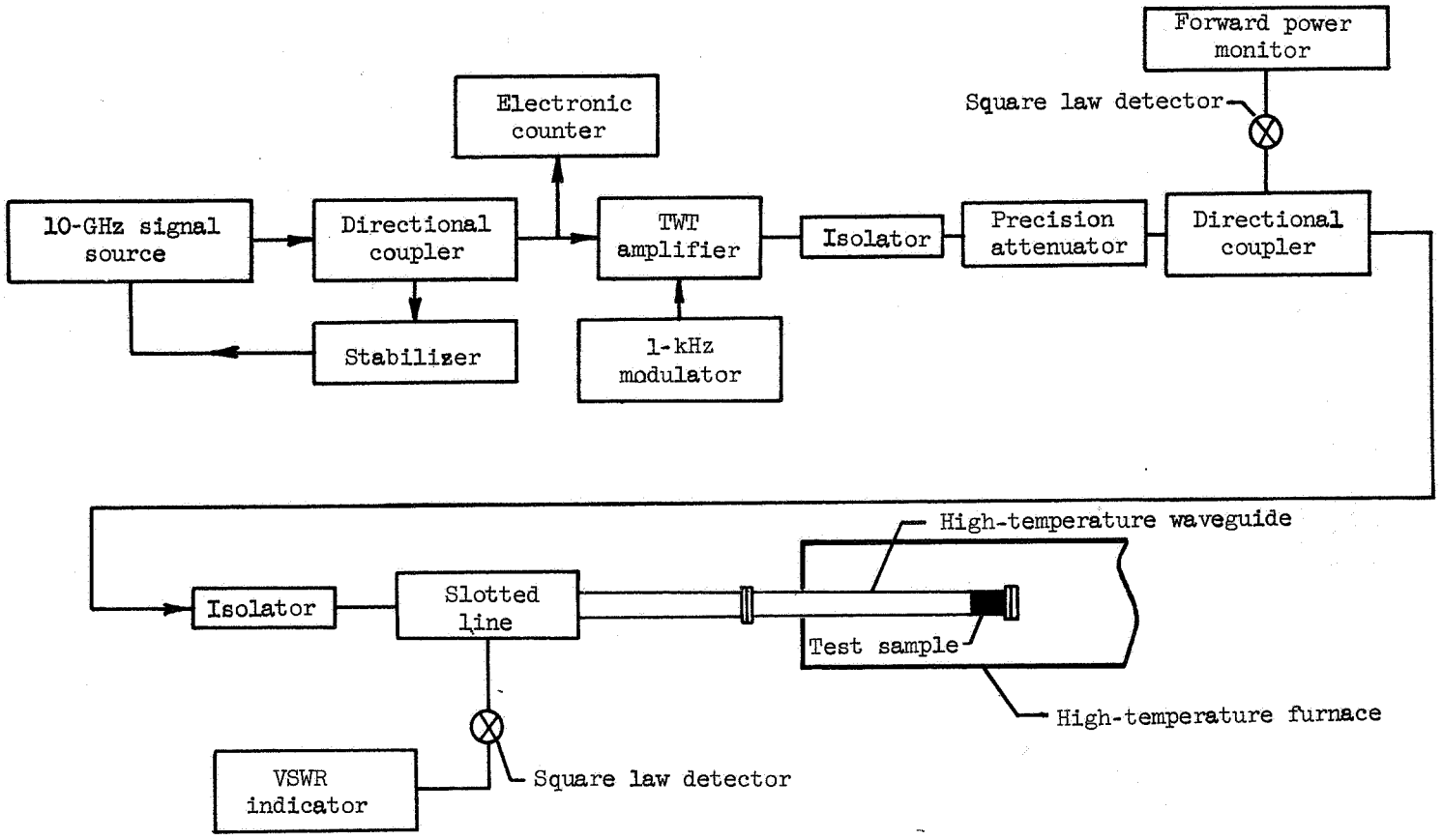

Figure 5.- Block diagram of instrumentation for high-temperature-materials measurements.

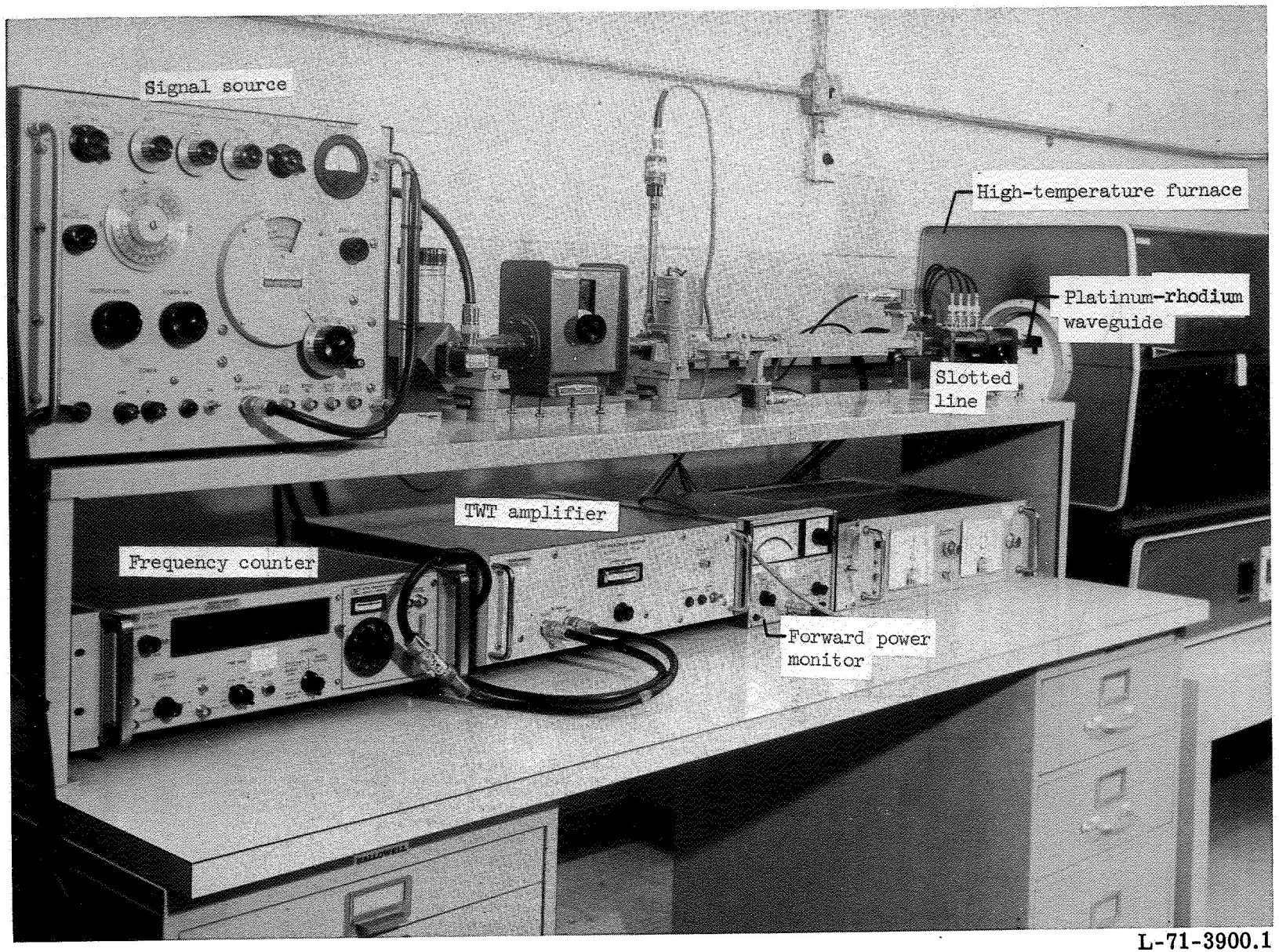

L-71-3900.1

Figure 6.- High-temperature-materials measurement facility.

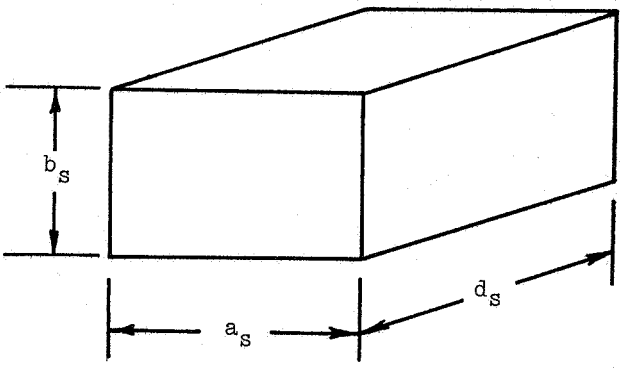

Figure 7.- Test sample configuration.

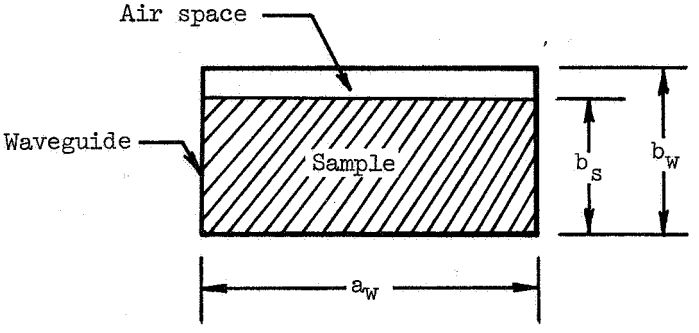

Figure 8.- Clearance between dielectric sample and waveguide.

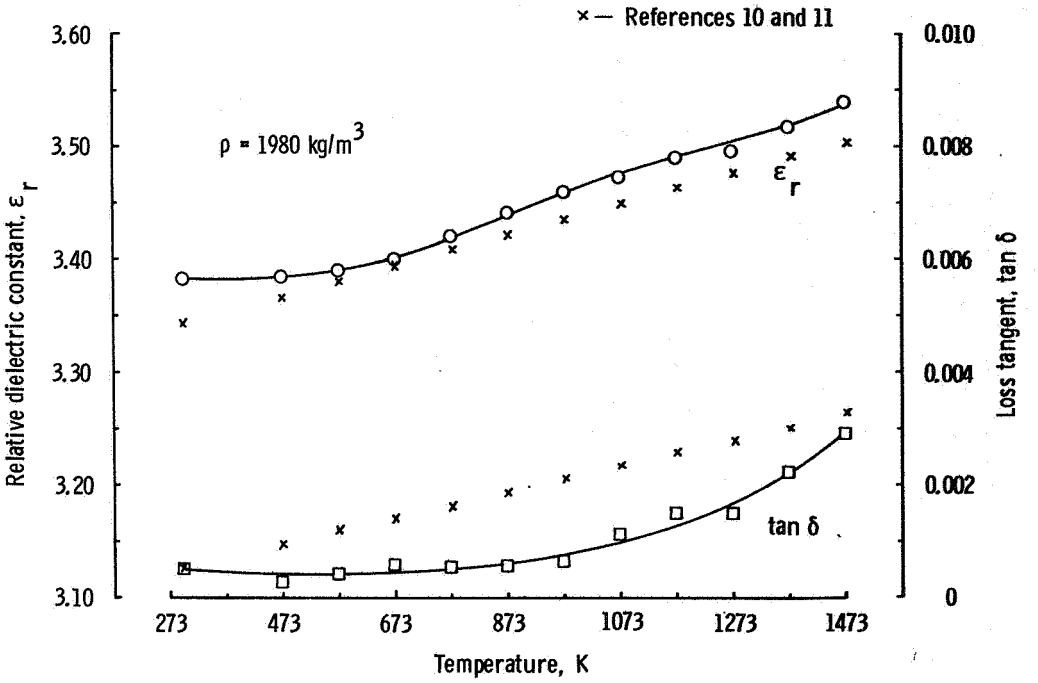

(a) Slip-cast fused silica (SCFS).

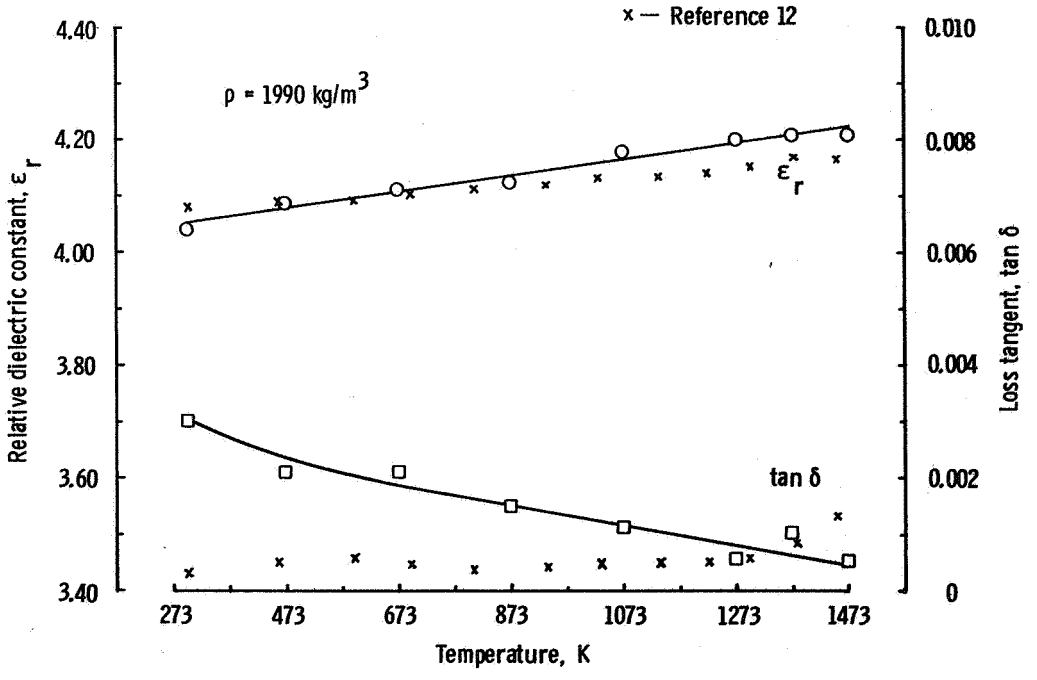

(b) Hot pressed boron nitride (HD-0092).

Figure 9.- Dielectric properties of candidate space shuttle materials as a function of temperature at a frequency of 10 GHz.

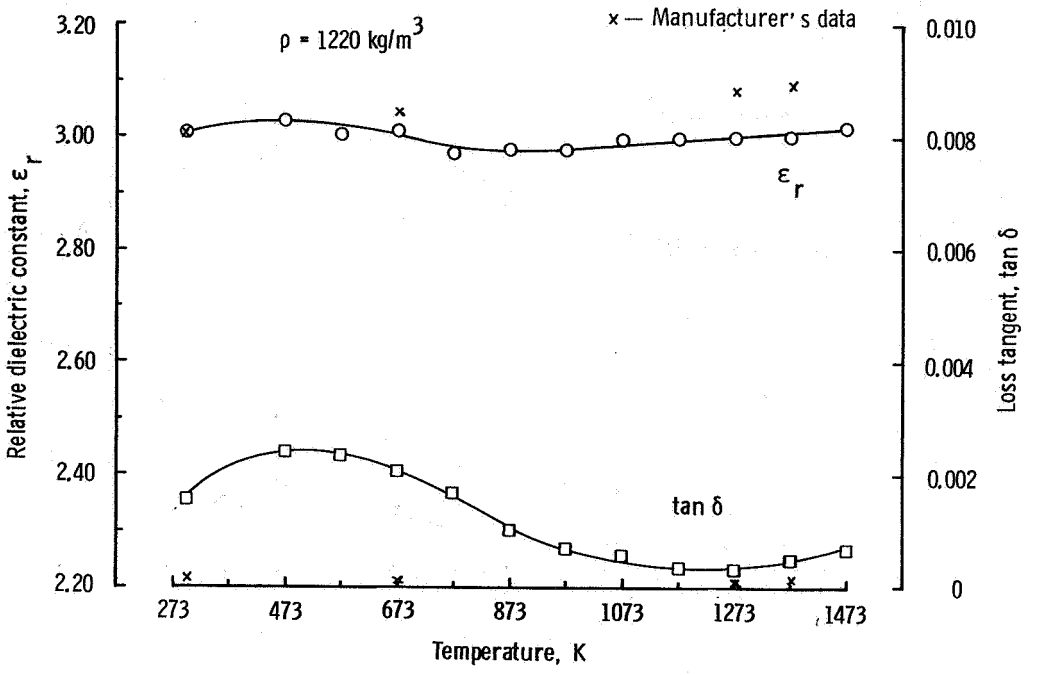

(c) Isotropic pyrolytic boron nitride (IPBN).

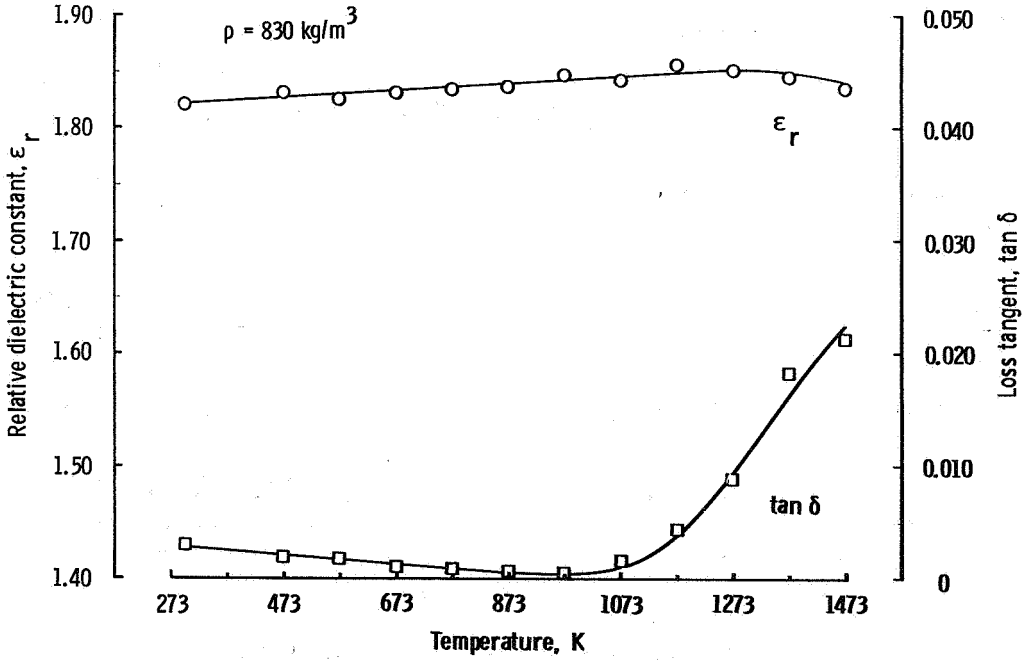

(d) Aluminum phosphate foam ($AlPO_4$).

Figure 9.- Continued.

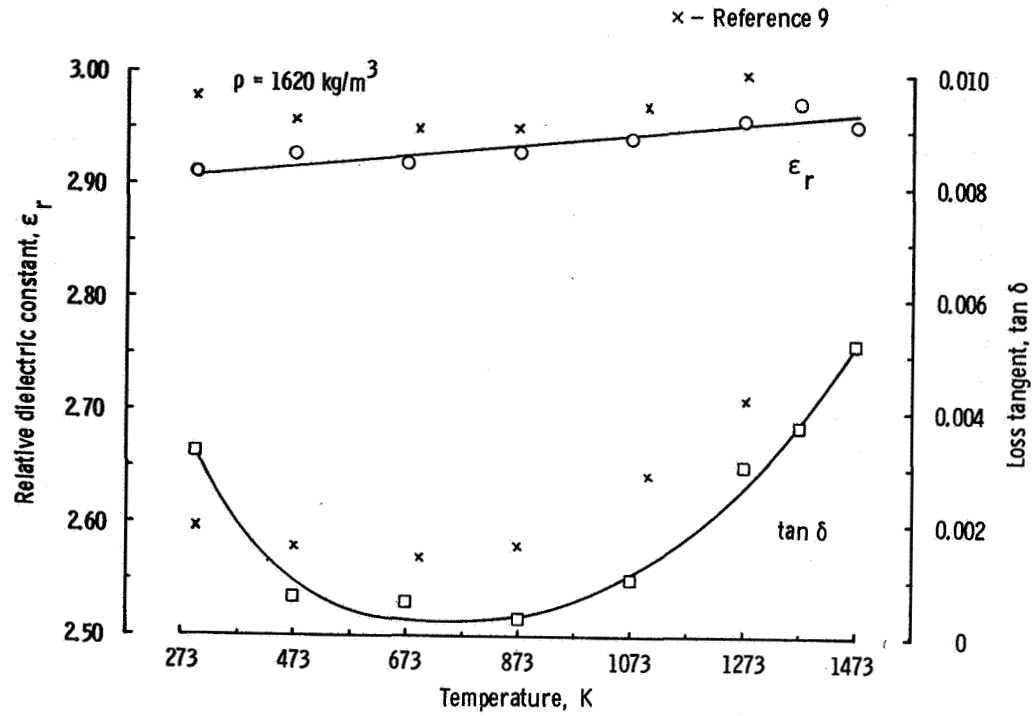

(e) Fused quartz reinforced silica composite (AS-3DX).

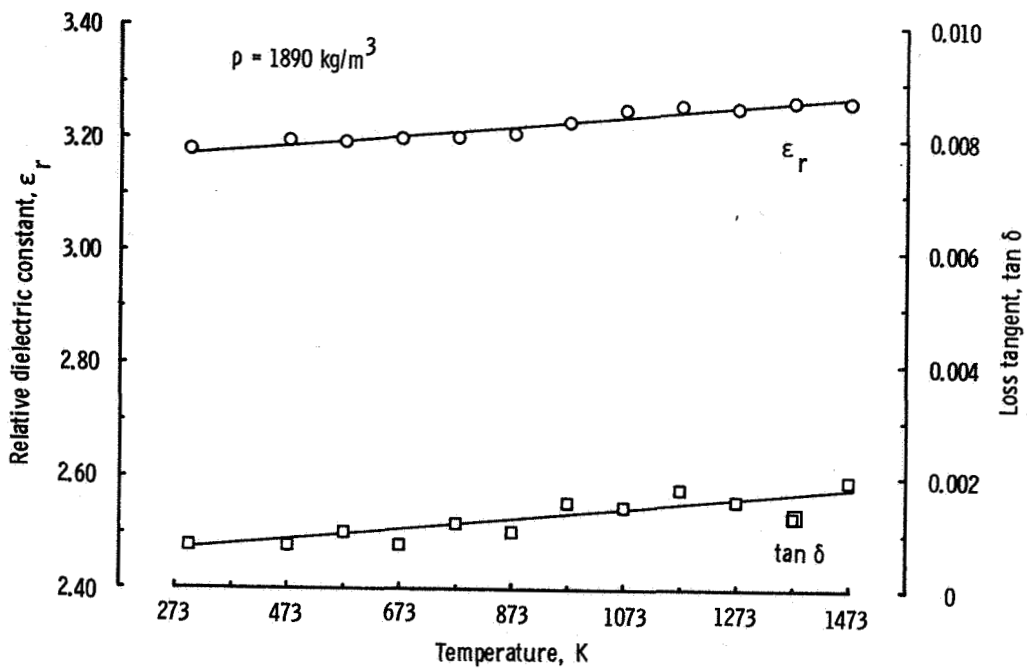

(f) Multidirectional silica composite (Markite 3DQ).

Figure 9.- Continued.

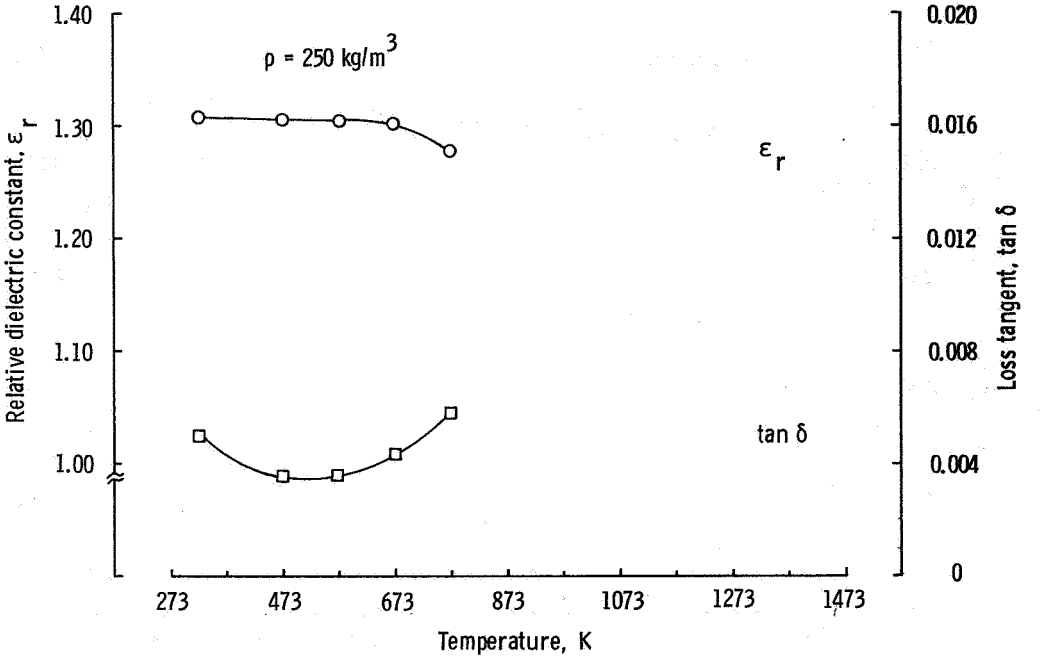

(g) Silicone ablator (SLA-220V H/C).

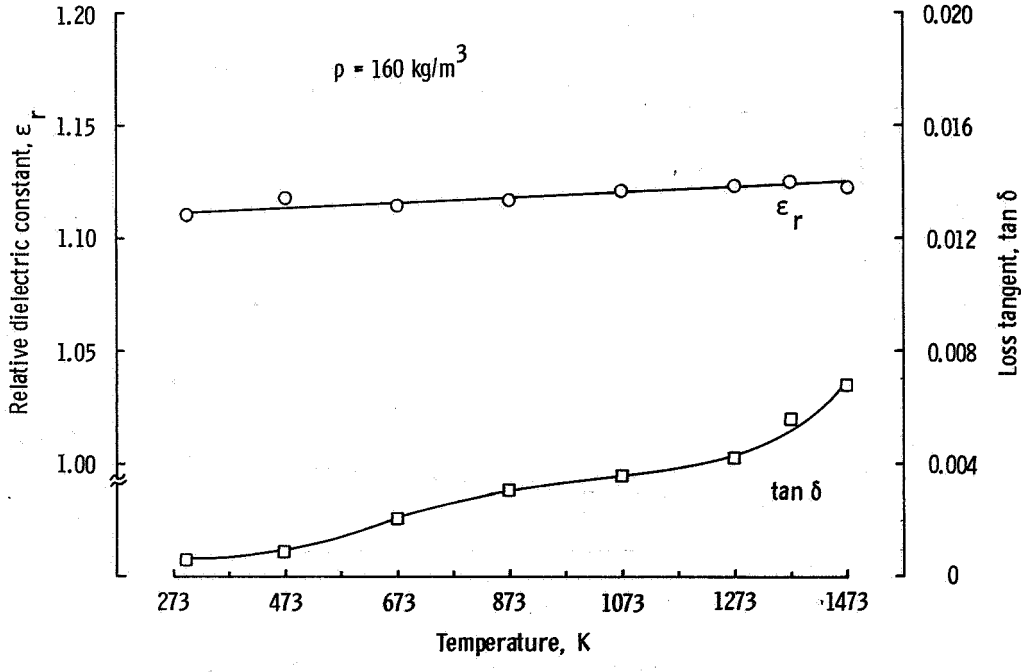

(h) Dynaquartz.

Figure 9.- Continued.

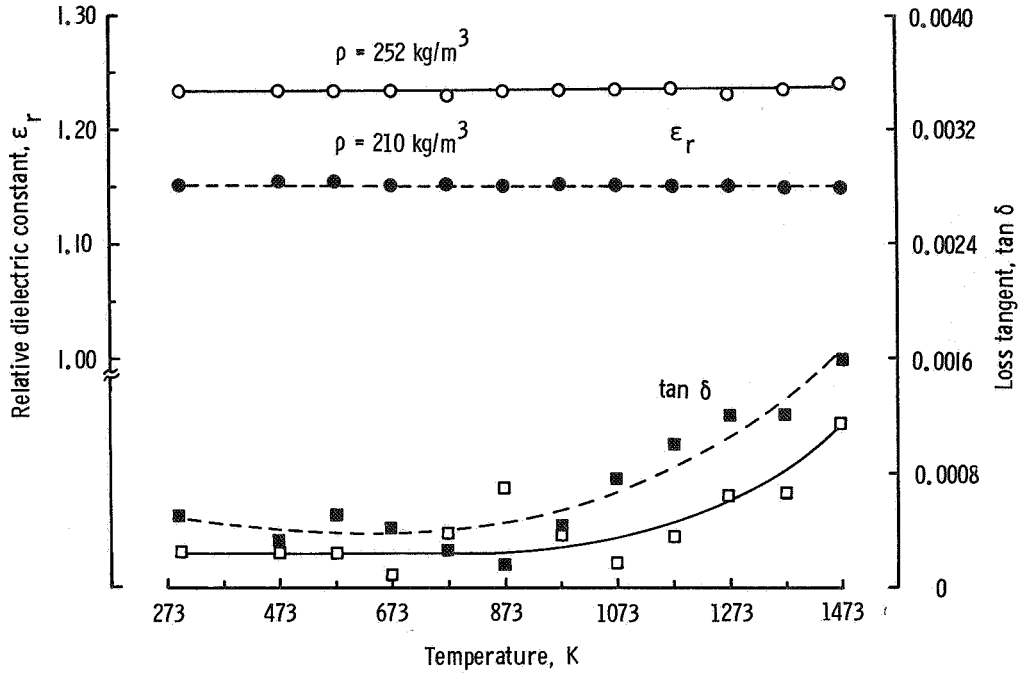

(i) All silica (LI-1500).

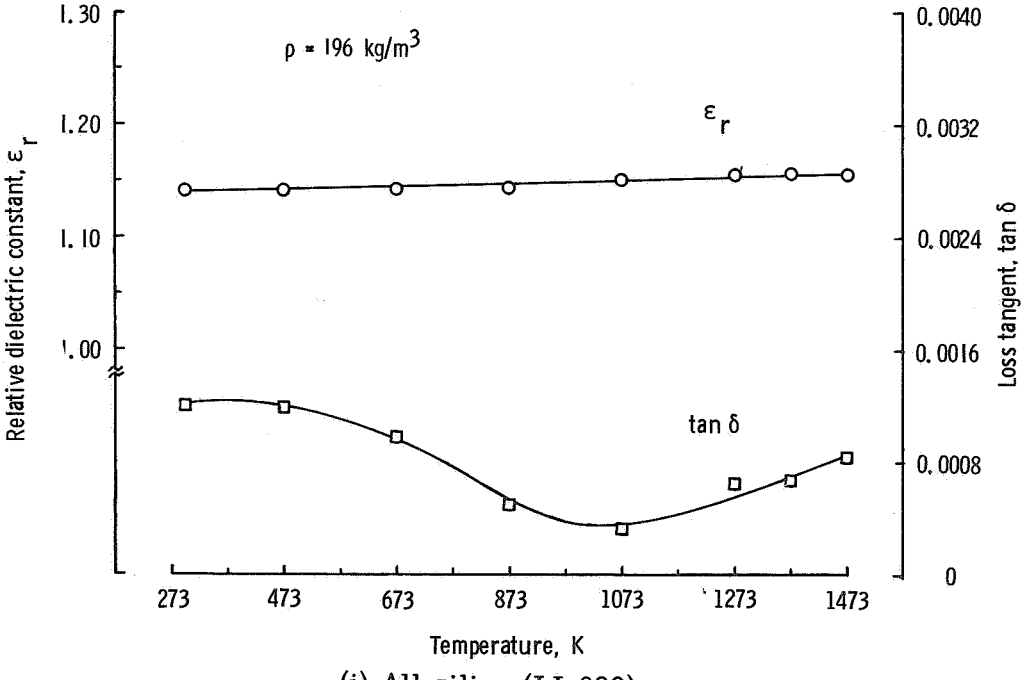

(j) All silica (LI-900).

Figure 9.- Continued.

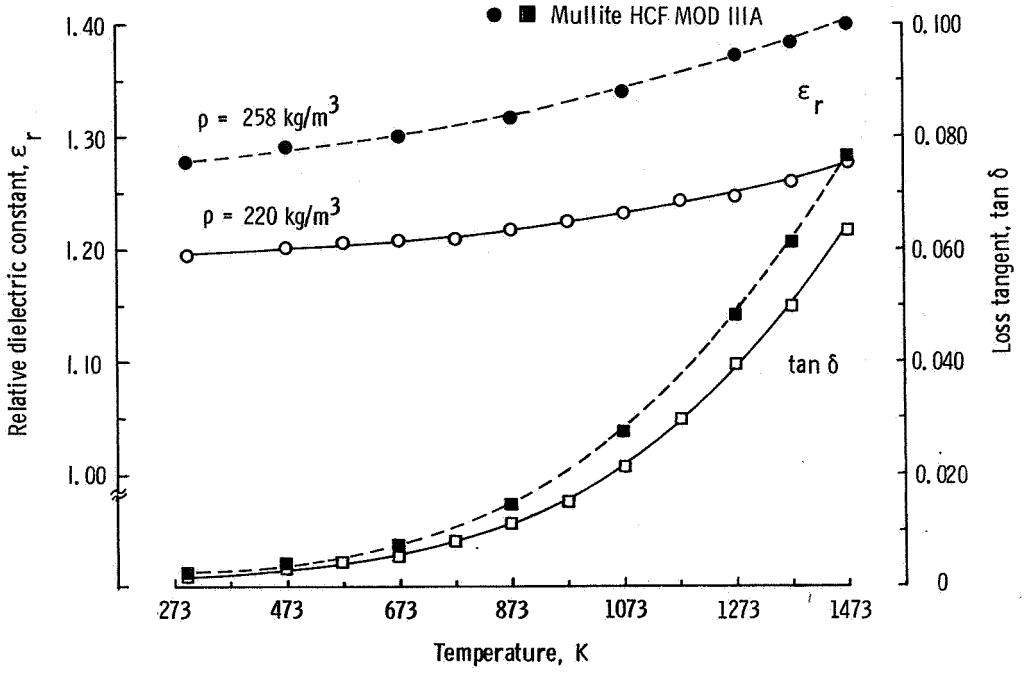

(k) Mullite HCF (hardened compacted fibers).

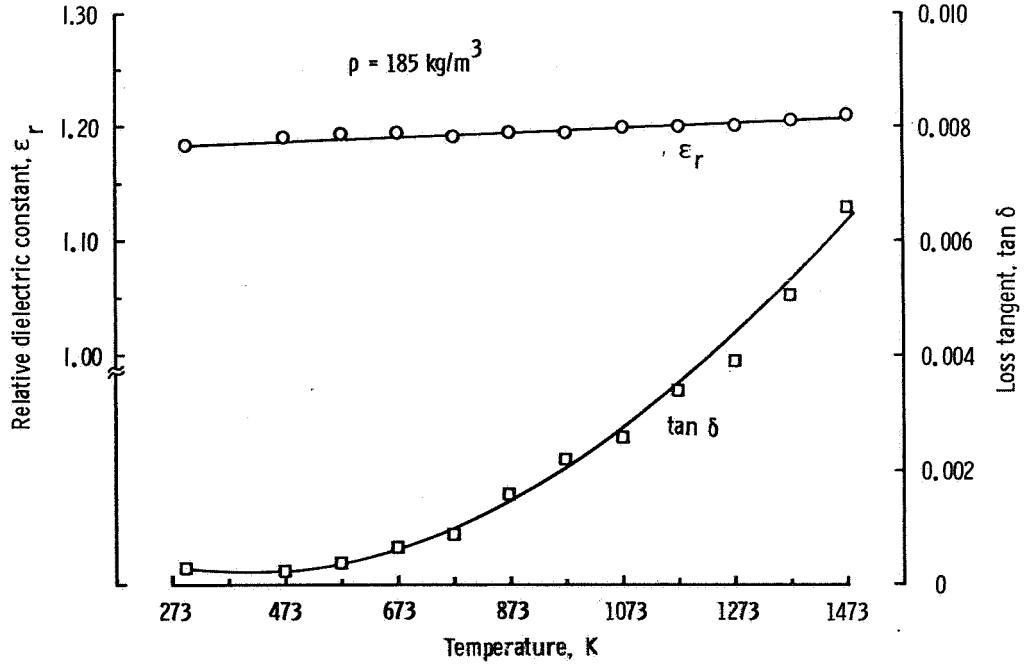

(l) Mullite MOD IA.

Figure 9.- Continued.

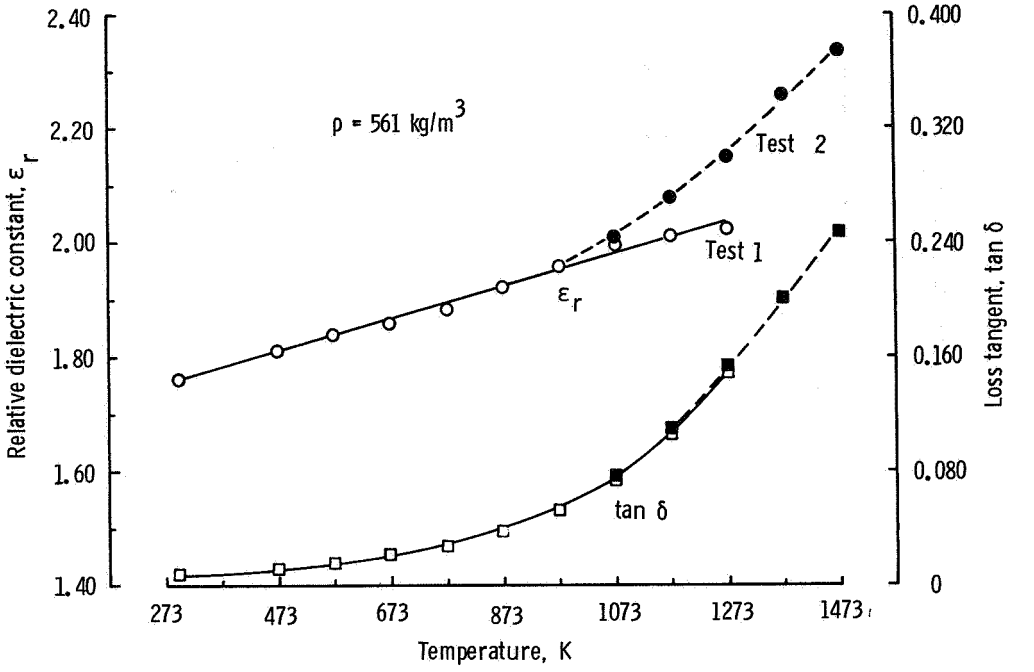

(m) Closed porosity insulation (CPI-35).

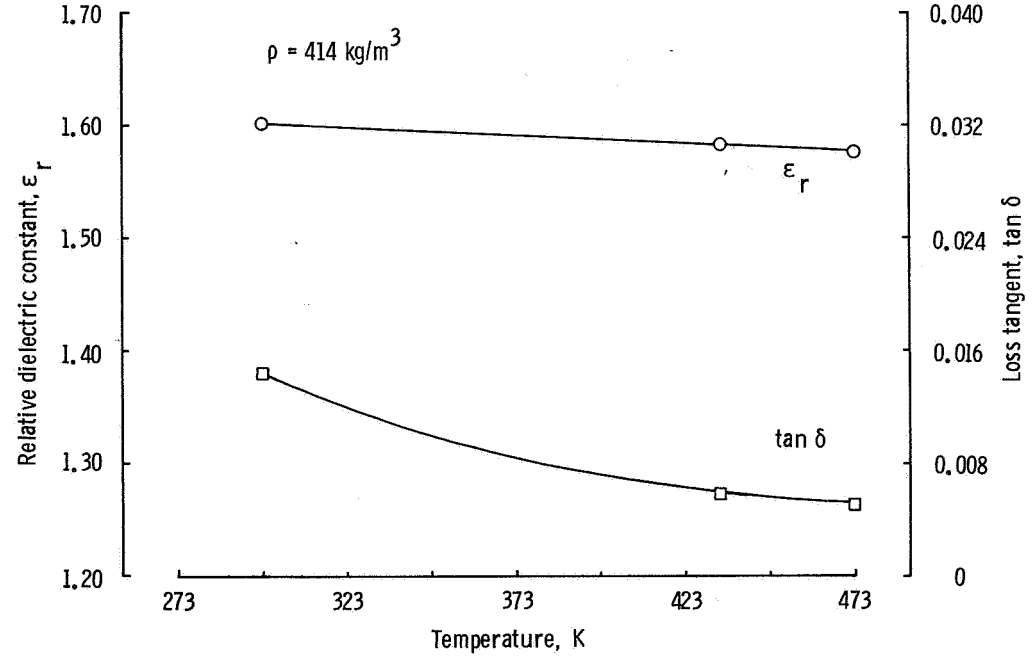

(n) Methyl phenyl silicone sponge (L-4350).

Figure 9.- Continued.

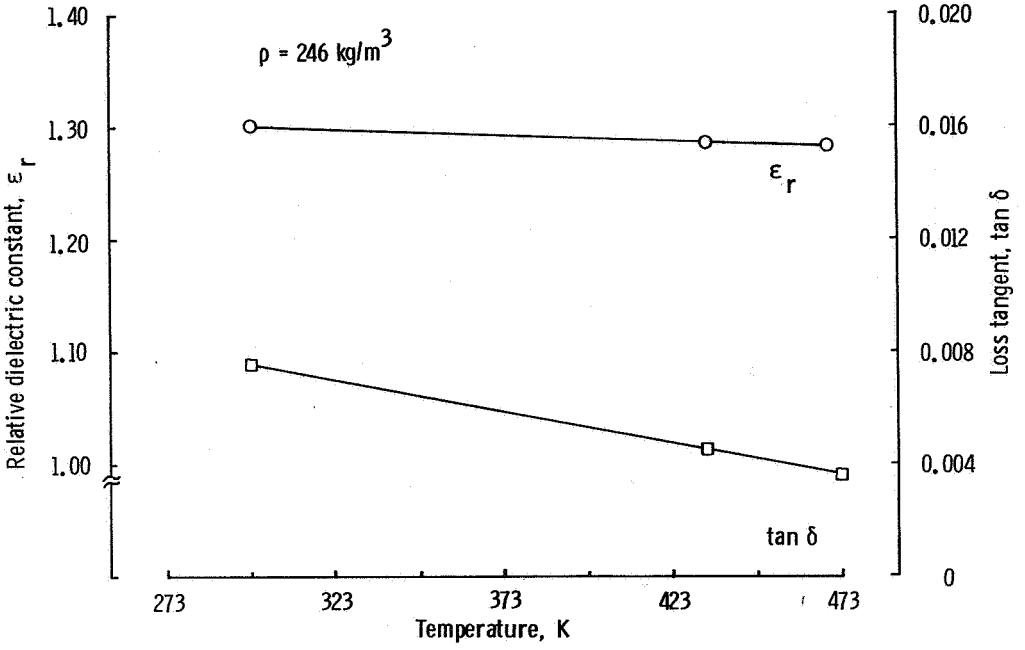

(o) Silicone sponge (RL-1973).

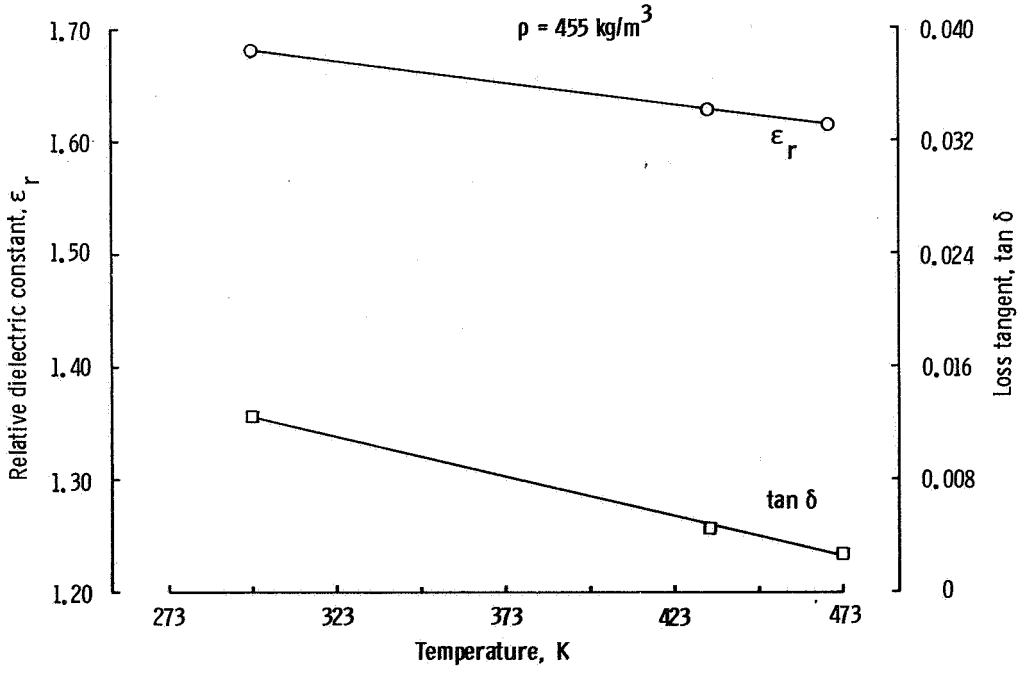

(p) Silicone sponge (S-105).

Figure 9.- Continued.

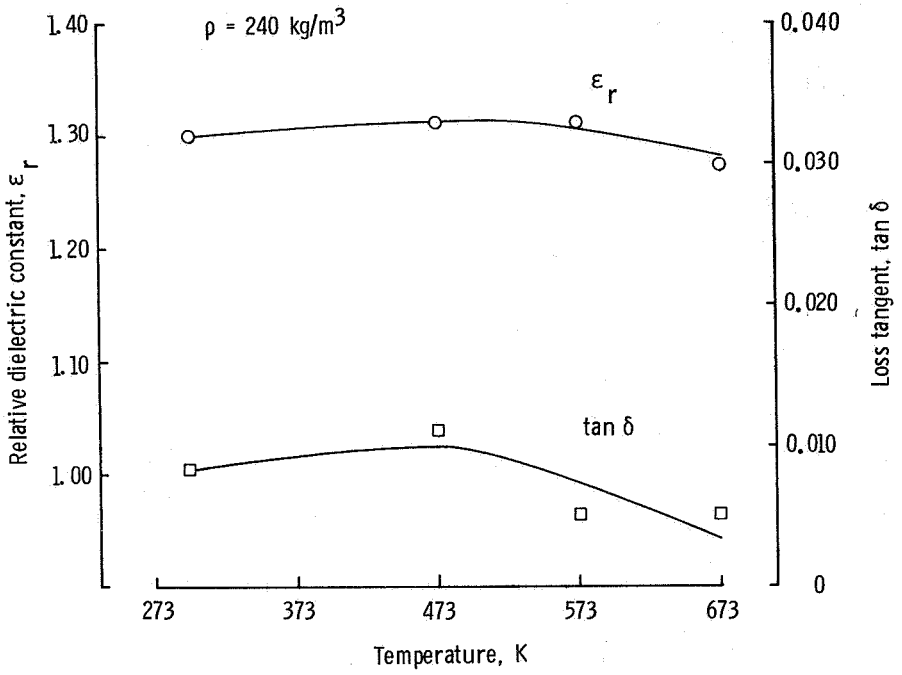

(q) Cork composite (SLA-561V H/C).

Figure 9.- Concluded.

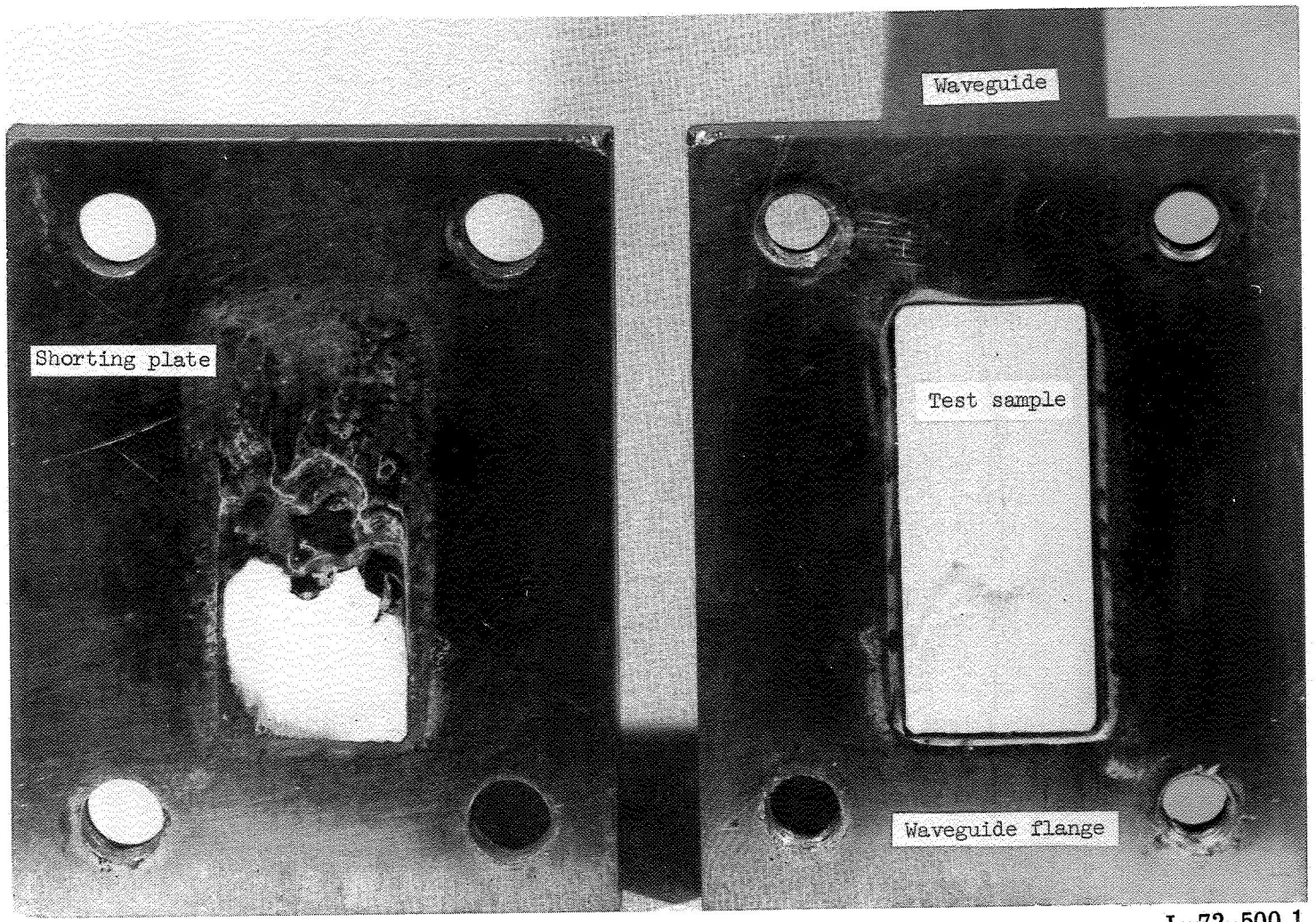

Figure 10.- High-temperature waveguide with boron nitride HD-0092 test sample after high-temperature test.

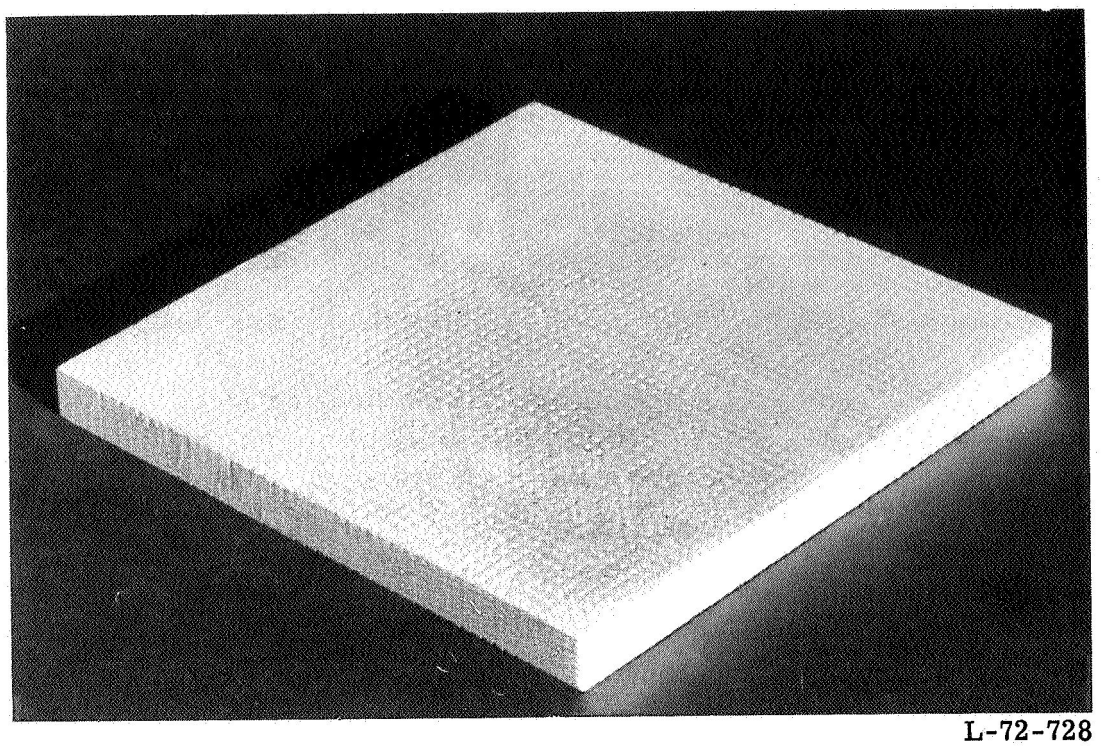

L-72-728

(a) Fused quartz reinforced silica composite (AS-3DX).

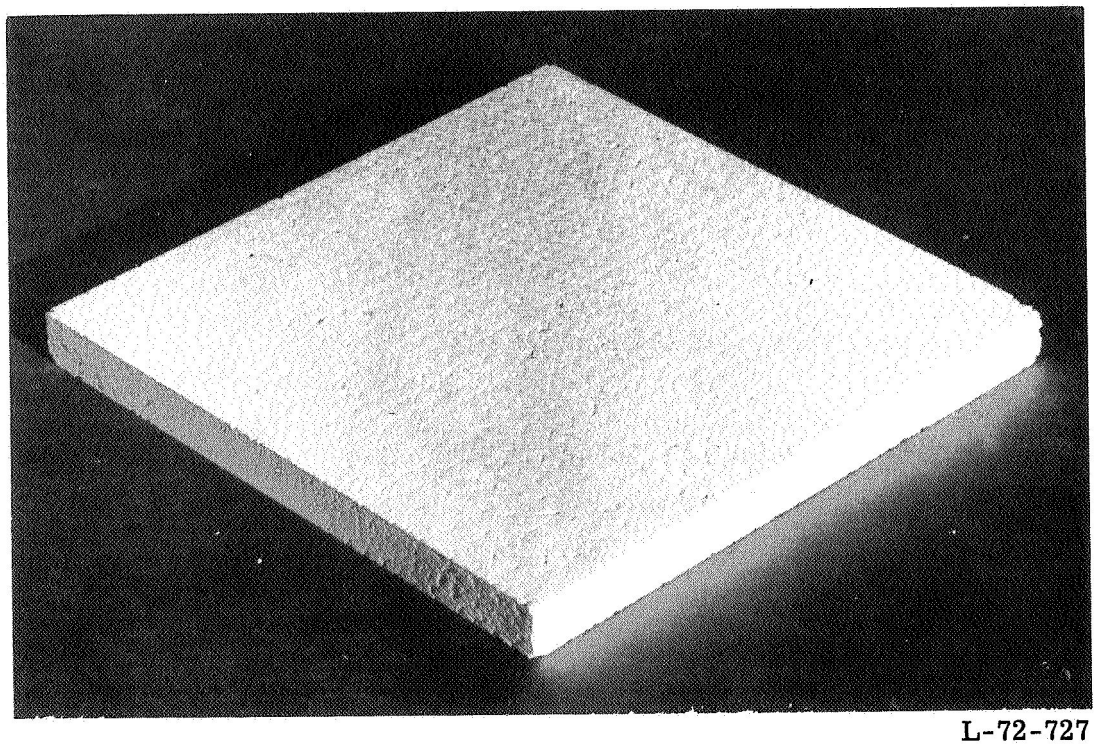

L-72-727

(b) Multidirectional silica composite (Markite 3DQ).

Figure 11.- Silica composite materials.

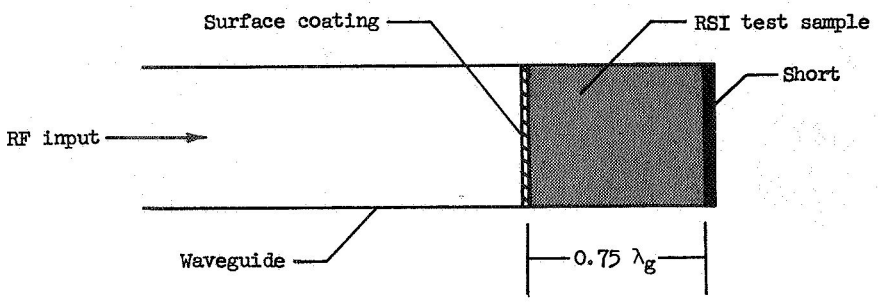

Figure 12.- Sketch of short-circuited waveguide with RSI test sample.

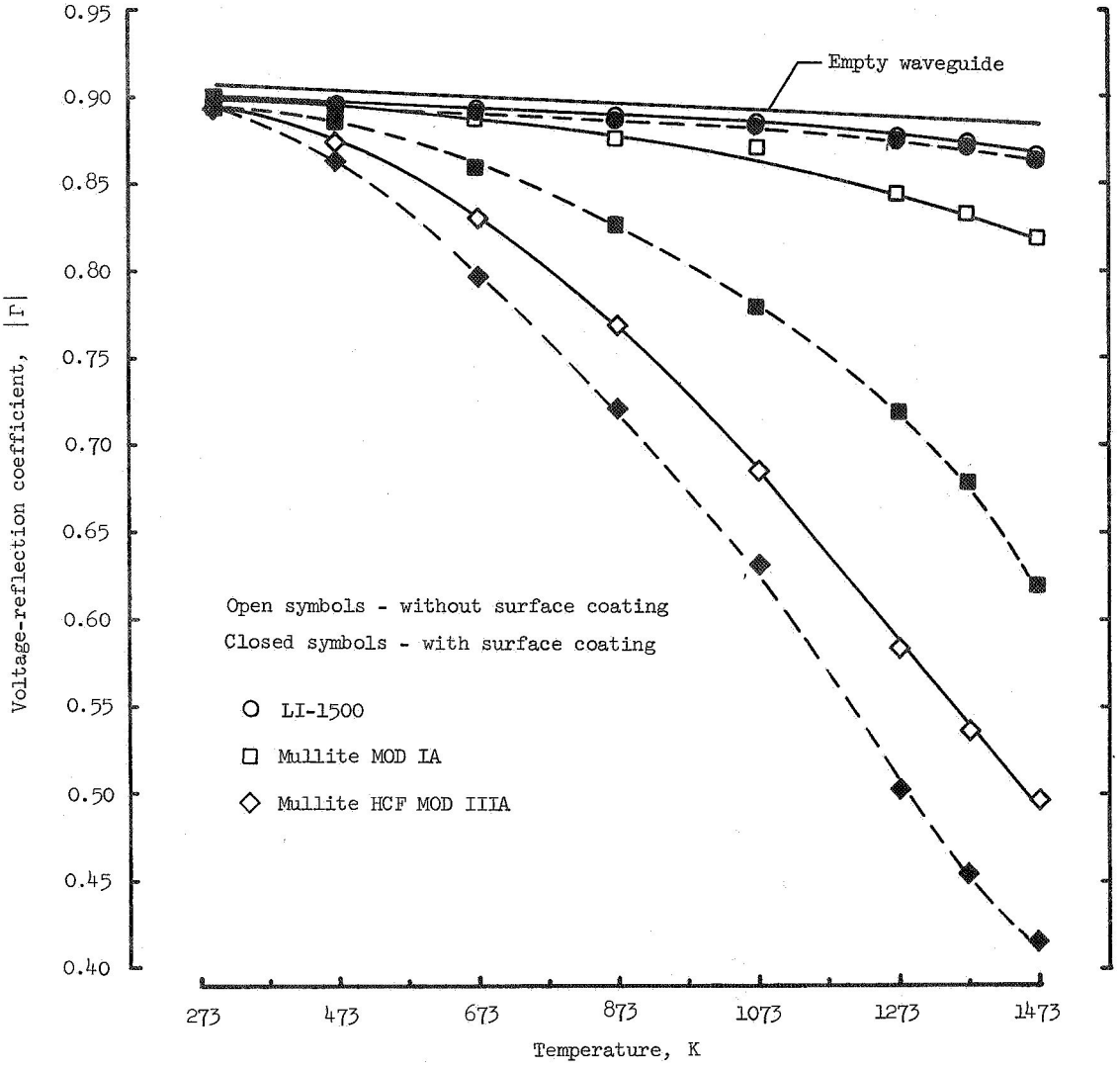

Figure 13.- Transmission properties of RSI surface coatings as a function of temperature at 10 GHz.

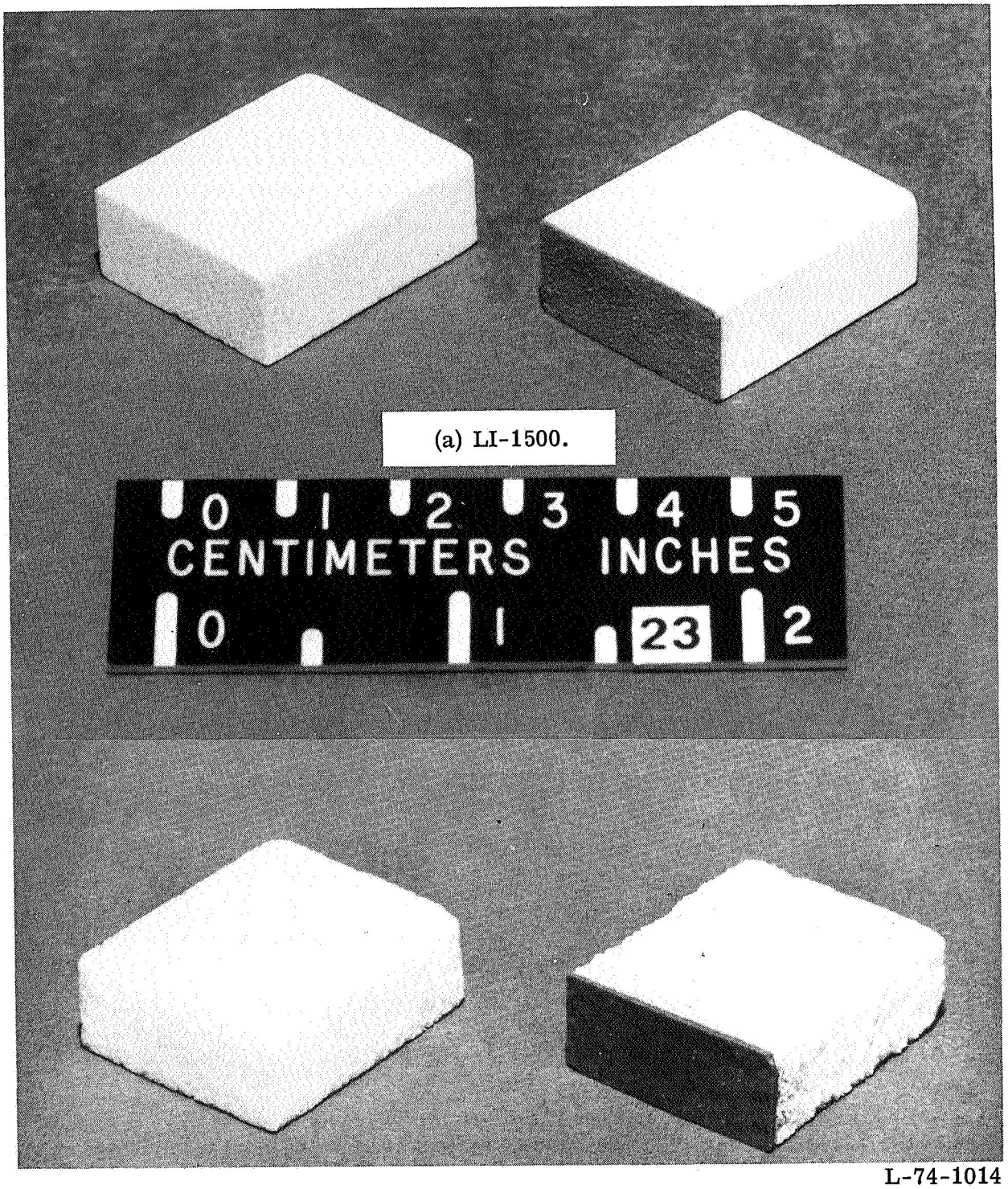

(b) Mullite MOD IA.

Figure 14.- RSI test samples with and without surface coatings.

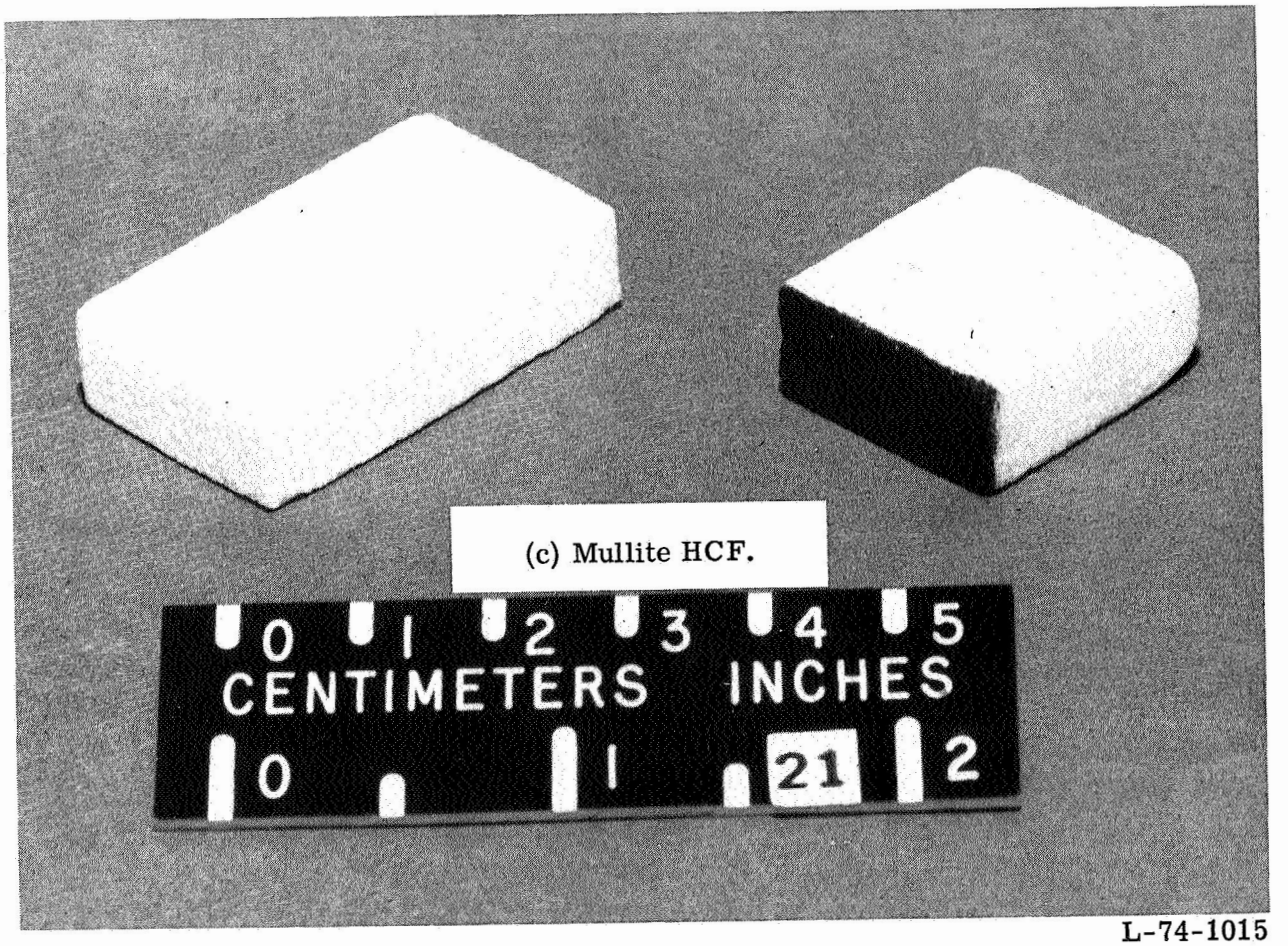

L-74-1015

Figure 14.- Concluded.

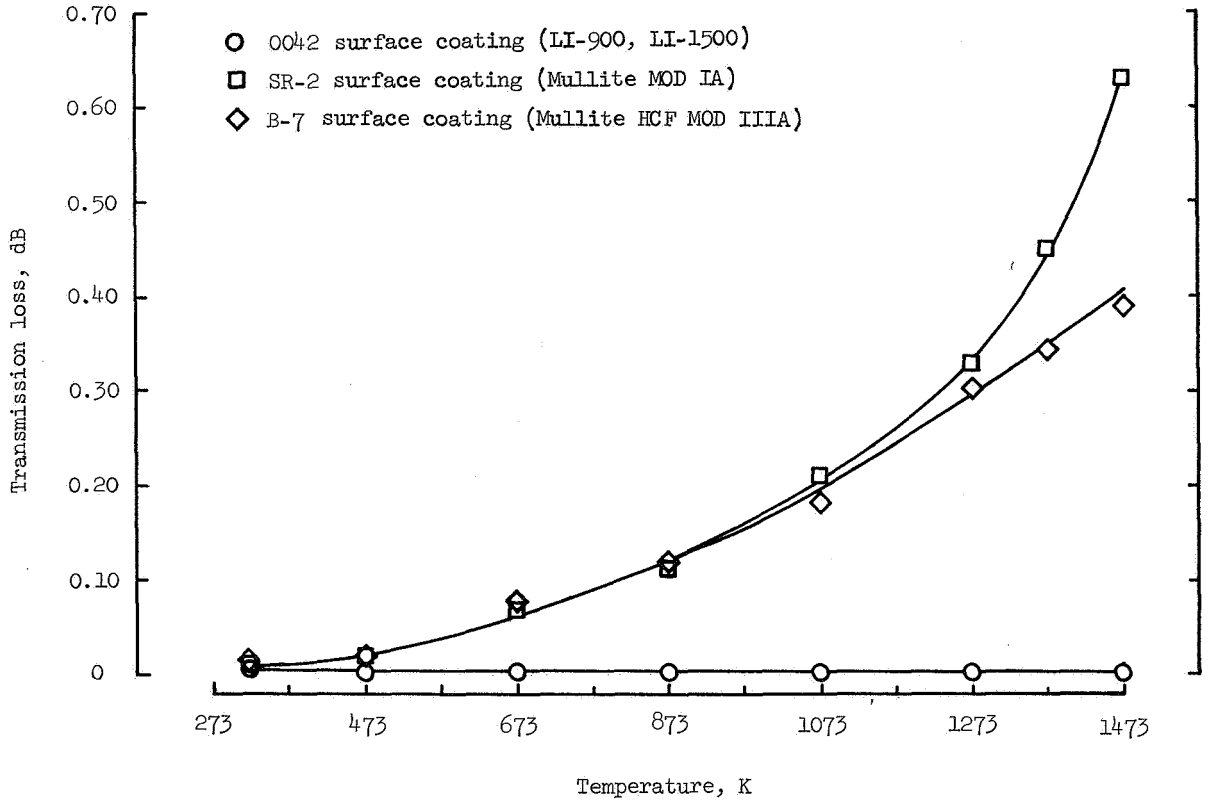

Figure 15.- Transmission loss of RSI surface coatings as a function of temperature at 10 GHz.

NATIONAL AERONAUTICS AND SPACE ADMINISTRATION
WASHINGTON, D.C. 20546

OFFICIAL BUSINESS
PENALTY FOR PRIVATE USE $300

SPECIAL FOURTH-CLASS RATE BOOK

POSTAGE AND FEES PAID
NATIONAL AERONAUTICS AND SPACE ADMINISTRATION
451

U.S.MAIL

POSTMASTER: If Undeliverable (Section 158 Postal Manual) Do Not Return

"The aeronautical and space activities of the United States shall be conducted so as to contribute . . . to the expansion of human knowledge of phenomena in the atmosphere and space. The Administration shall provide for the widest practicable and appropriate dissemination of information concerning its activities and the results thereof."

—NATIONAL AERONAUTICS AND SPACE ACT OF 1958

NASA SCIENTIFIC AND TECHNICAL PUBLICATIONS

TECHNICAL REPORTS: Scientific and technical information considered important, complete, and a lasting contribution to existing knowledge.

TECHNICAL NOTES: Information less broad in scope but nevertheless of importance as a contribution to existing knowledge.

TECHNICAL MEMORANDUMS: Information receiving limited distribution because of preliminary data, security classification, or other reasons. Also includes conference proceedings with either limited or unlimited distribution.

CONTRACTOR REPORTS: Scientific and technical information generated under a NASA contract or grant and considered an important contribution to existing knowledge.

TECHNICAL TRANSLATIONS: Information published in a foreign language considered to merit NASA distribution in English.

SPECIAL PUBLICATIONS: Information derived from or of value to NASA activities. Publications include final reports of major projects, monographs, data compilations, handbooks, sourcebooks, and special bibliographies.

TECHNOLOGY UTILIZATION PUBLICATIONS: Information on technology used by NASA that may be of particular interest in commercial and other non-aerospace applications. Publications include Tech Briefs, Technology Utilization Reports and Technology Surveys.

Details on the availability of these publications may be obtained from:

SCIENTIFIC AND TECHNICAL INFORMATION OFFICE

NATIONAL AERONAUTICS AND SPACE ADMINISTRATION

Washington, D.C. 20546